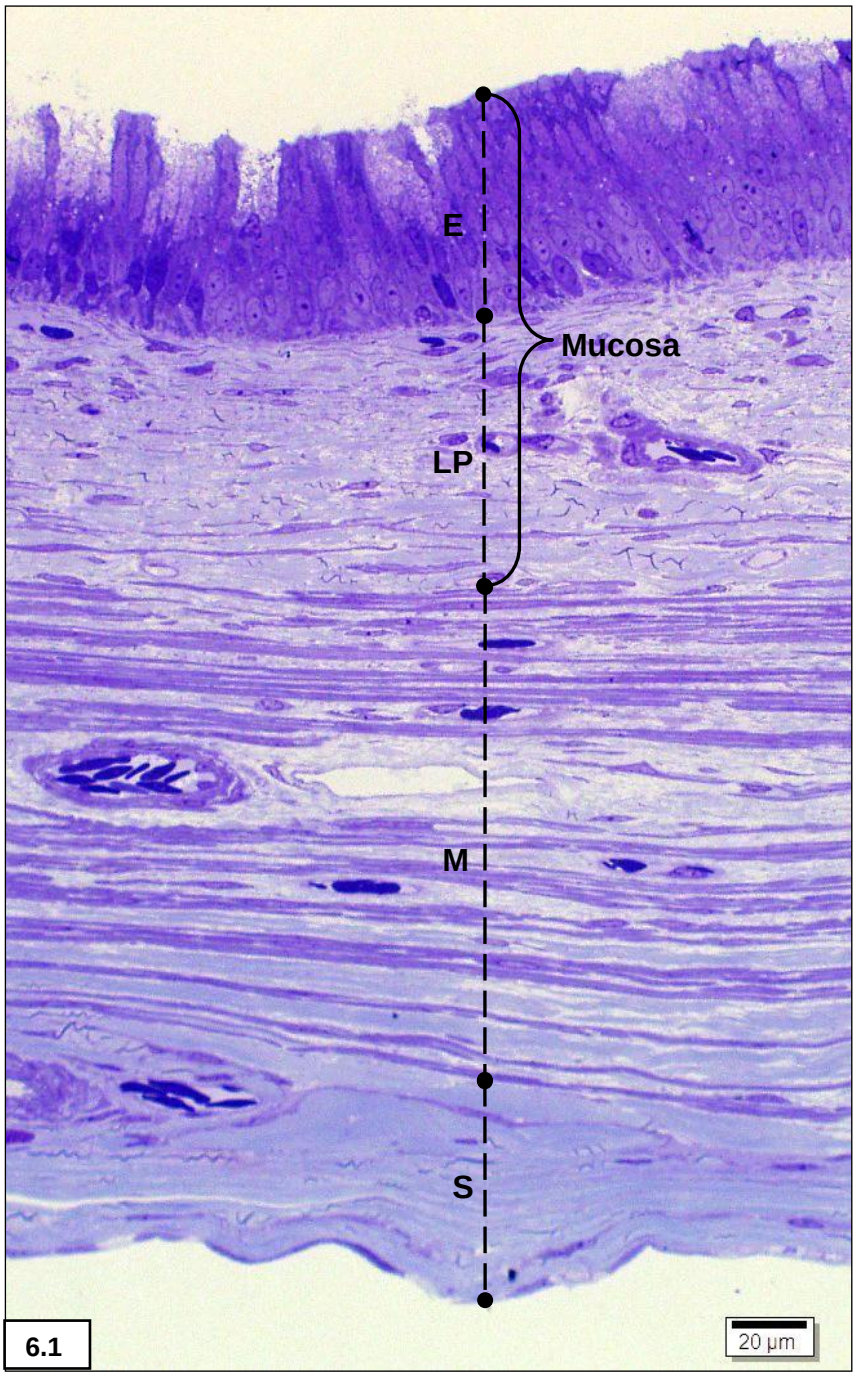

Figure 6.1: Toluidine blue (TB) resin section illustrating the full-thickness of the gallbladder wall: pseudostratified columnarv epithelium (**E**), *lamina propria* (**LP**), *muscularis externa* (**M**) and serosa including the subserosa (**S**).

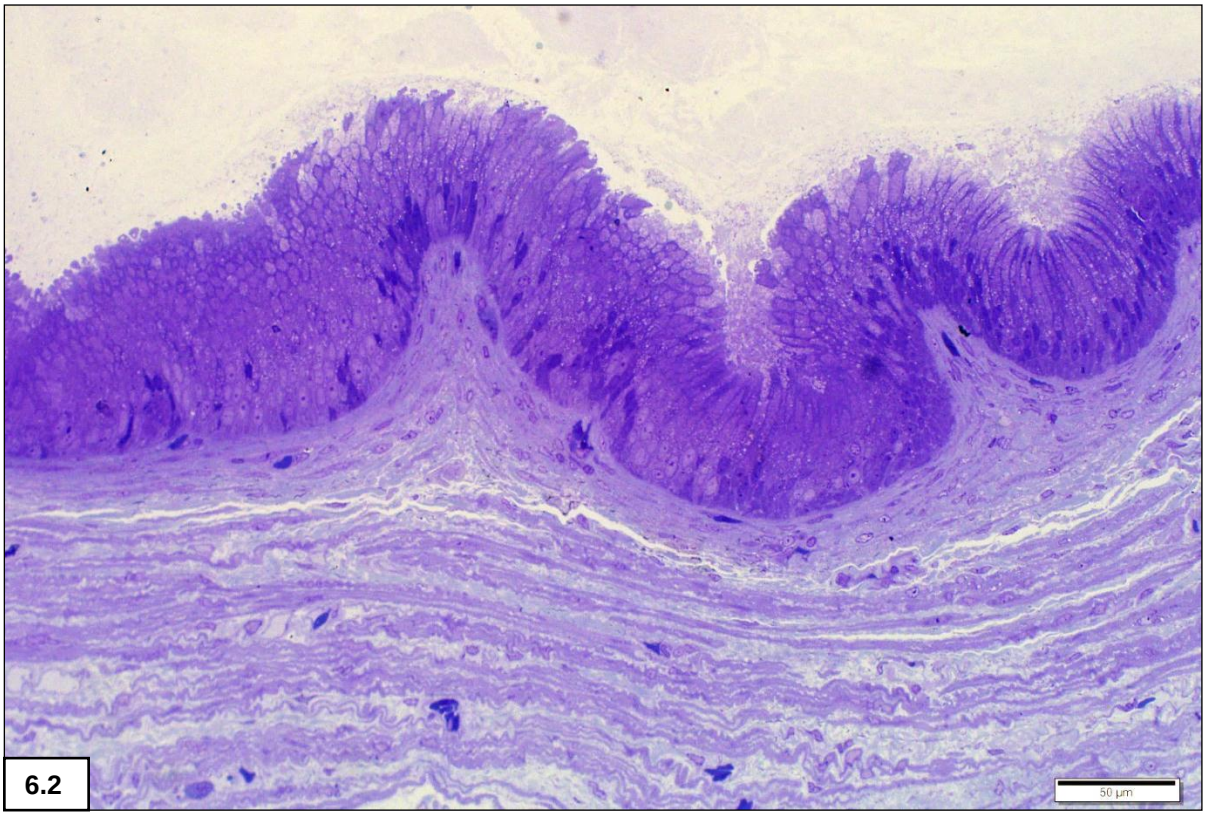

Figure 6.2: Pseudostratified columnar epithelium of the gallbladder mucosa showing irregular shallow folding. TB.

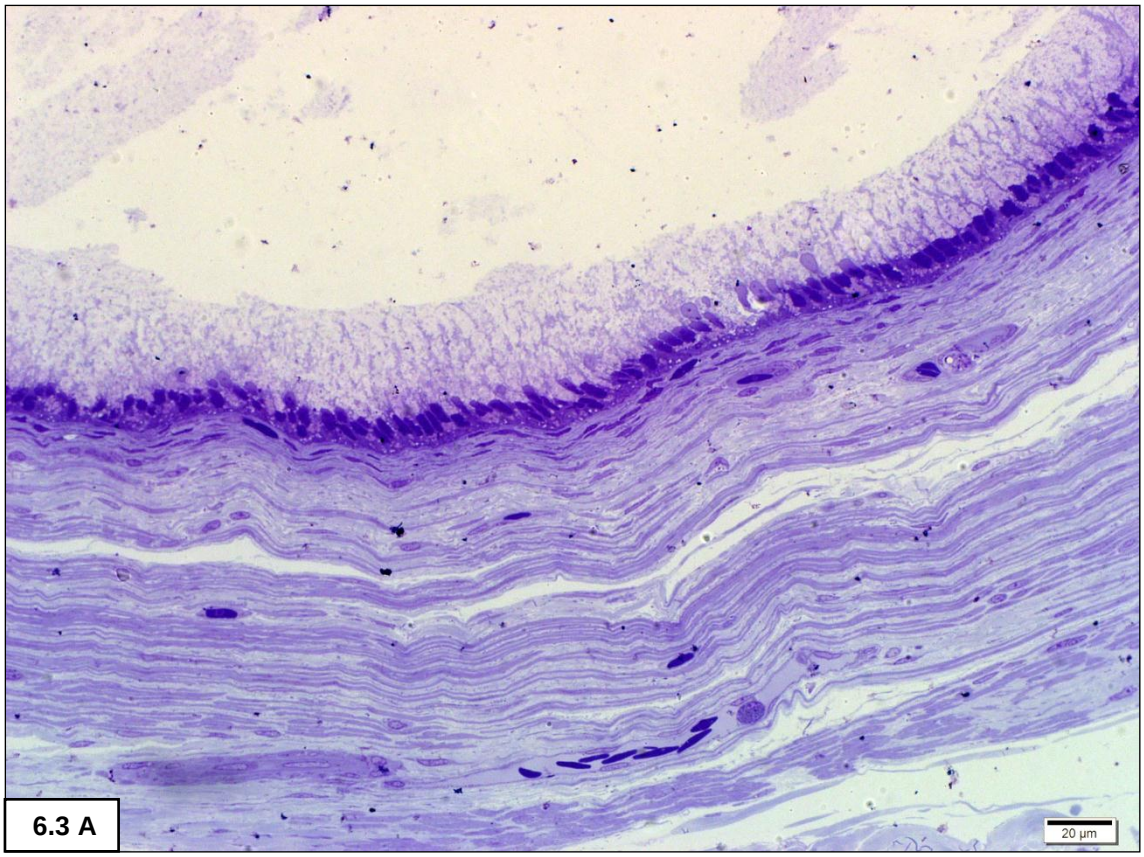

Figure 6.3 A: Putative simple columnar epithelium. TB.
B: Apparent merging of simple into pseudostratified columnar epithelium in two areas (brackets).TB.

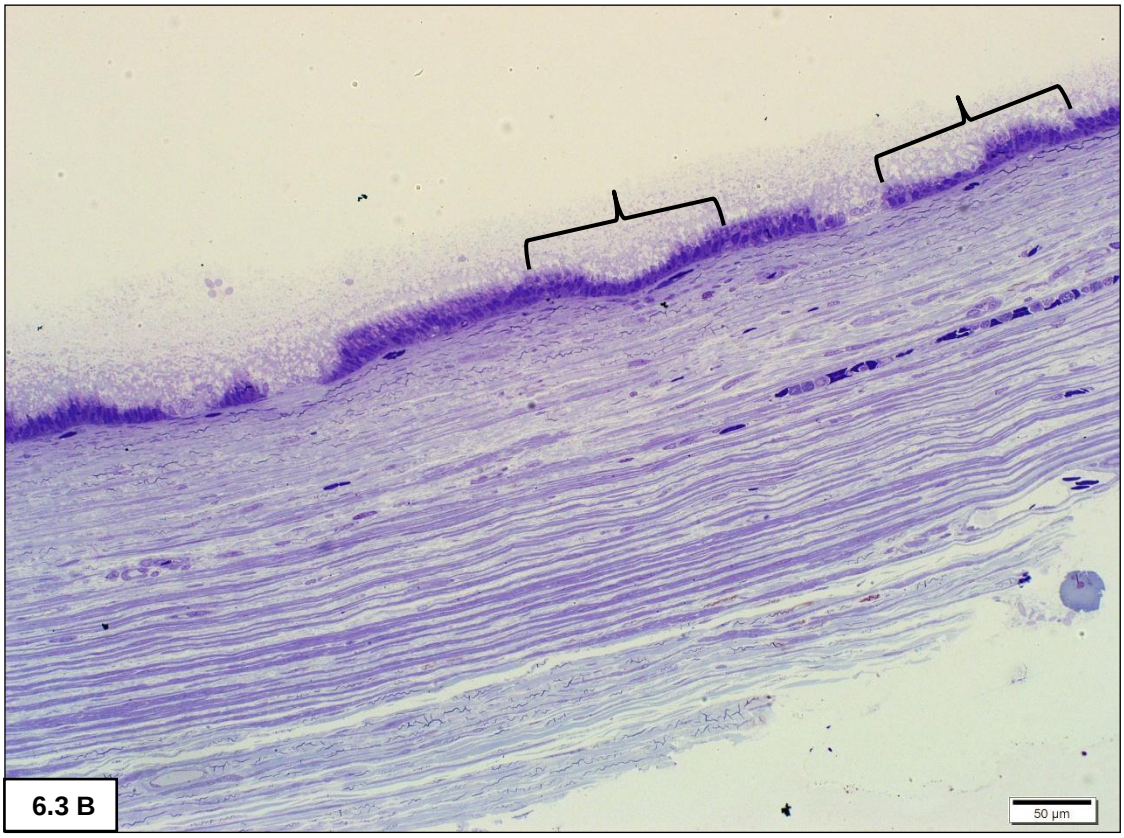

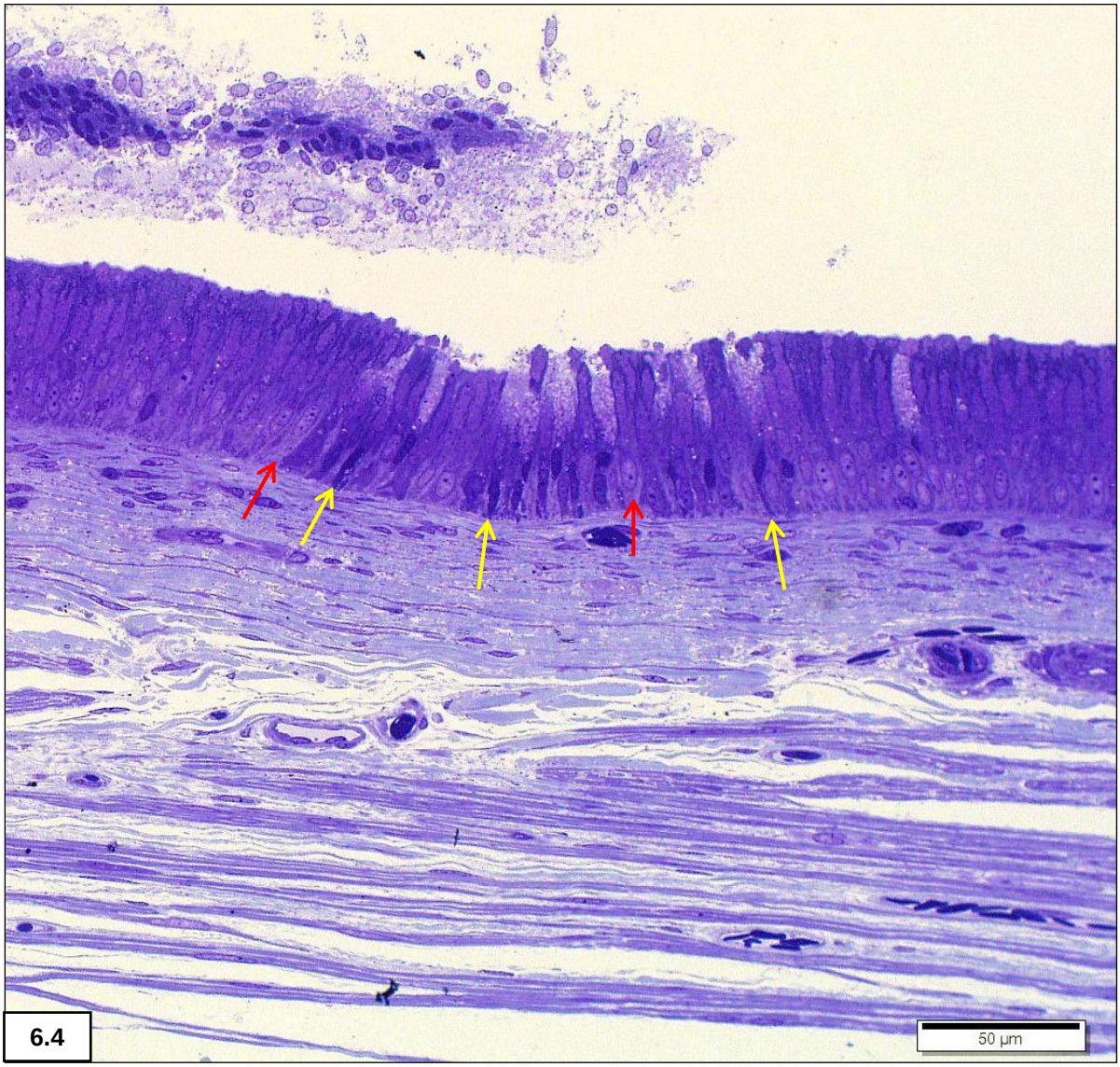

Figure 6.4: Pseudostratified columnar epithelium showing dark (yellow arrows) and light cells (red arrows). Note cellular debris in lumen. TB.

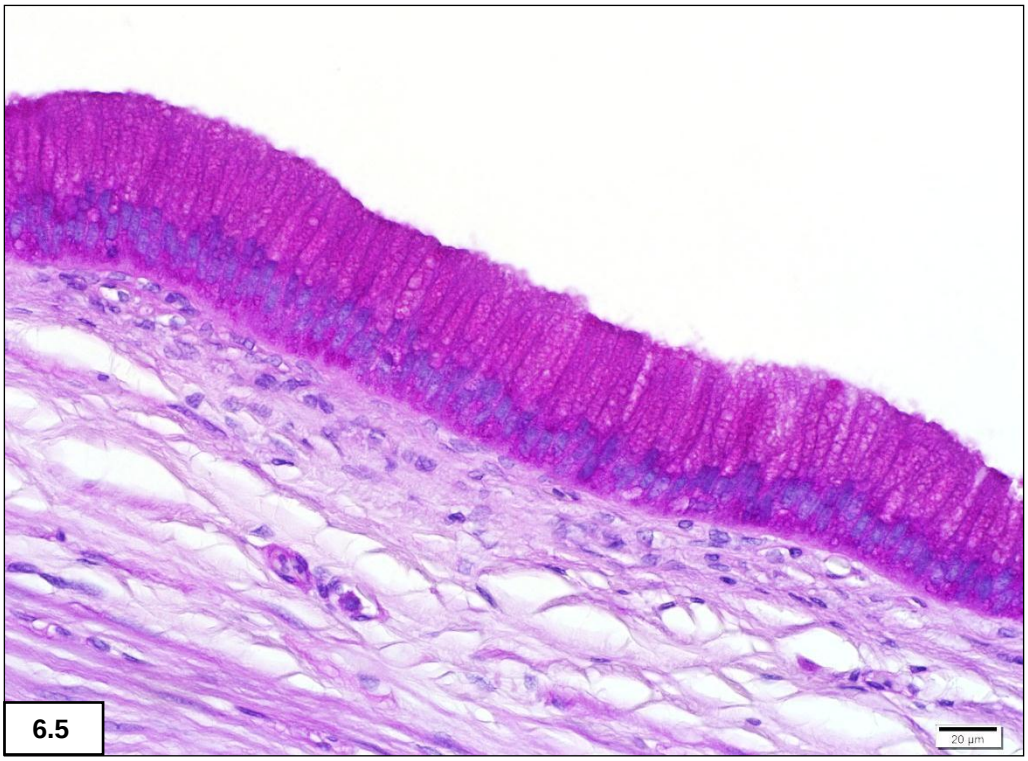

Figure 6.5: Slender goblet cells showing a PAS-positive staining reaction for carbohydrates in the apical and basal epithelial cytoplasm.

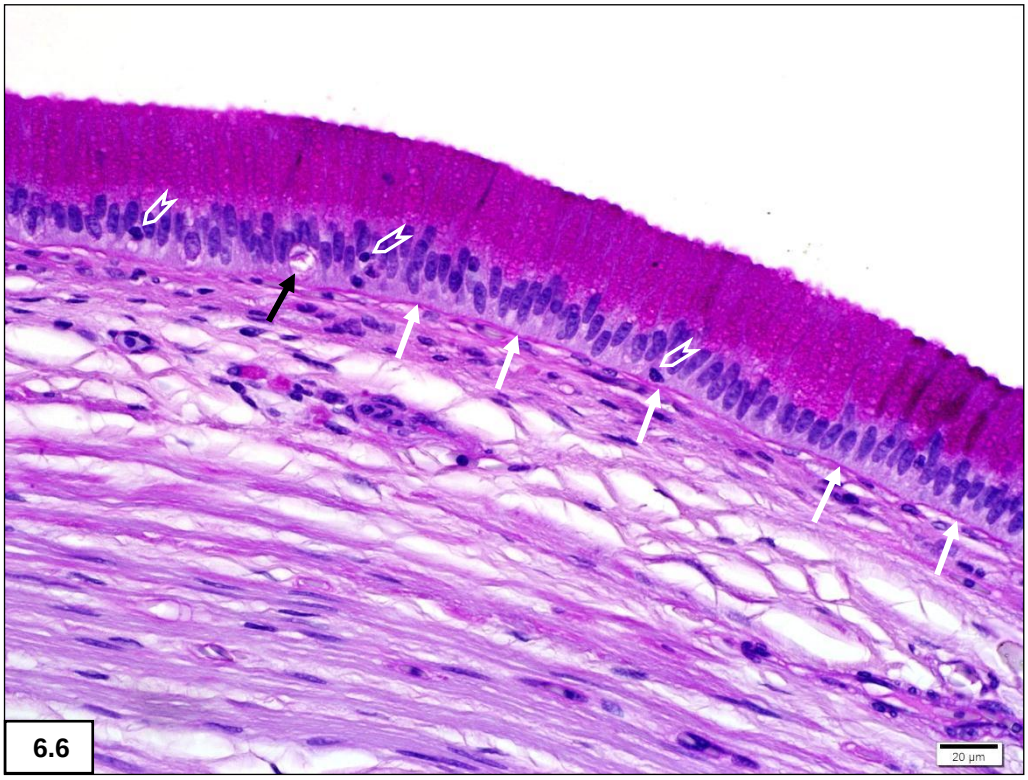

Figure 6.6: PAS staining reaction with diastase treatment illustrating the removal of glycogen in the basal regions with mucus positivity remaining in the apical portions. Note the pink-staining basement membrane (white arrows), vacuole (black arrow) and epithelial lymphocytes (arrowheads).

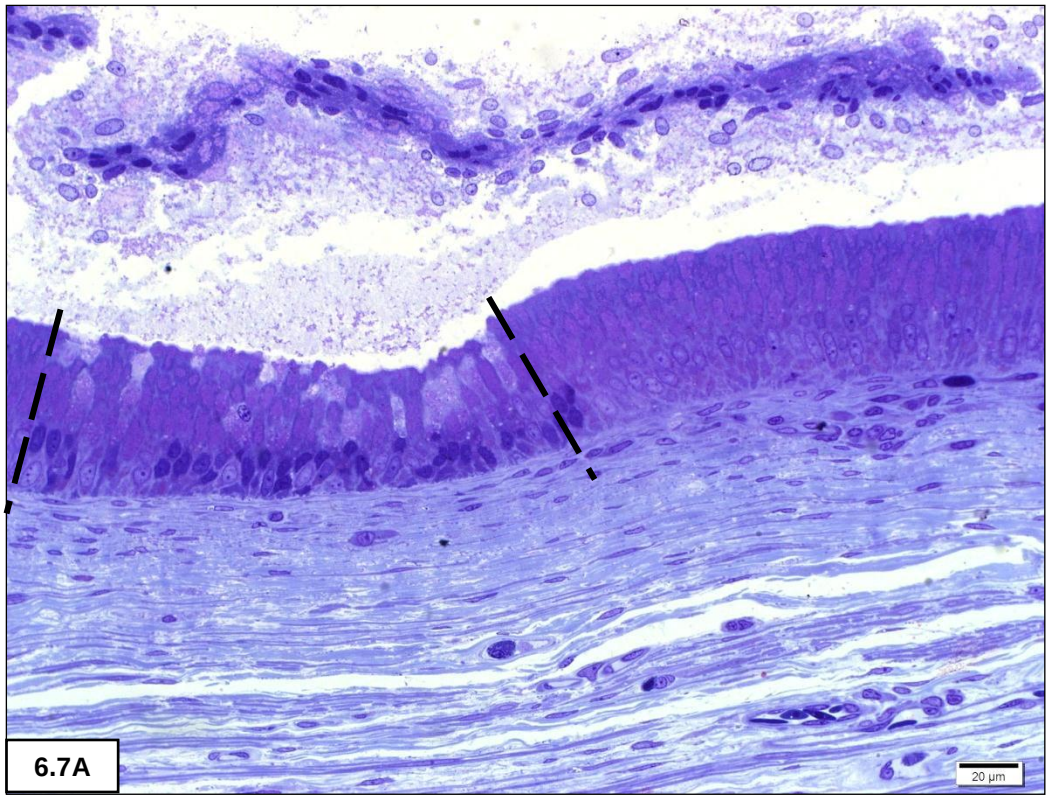

Figure 6.7A: Epithelium in initial secretory phase or recovery phase (between dashed lines) adjacent to “resting” epithelium. Note the increase in dark cells in this area. Cellular debris and mucous remnants are evident in the lumen. TB

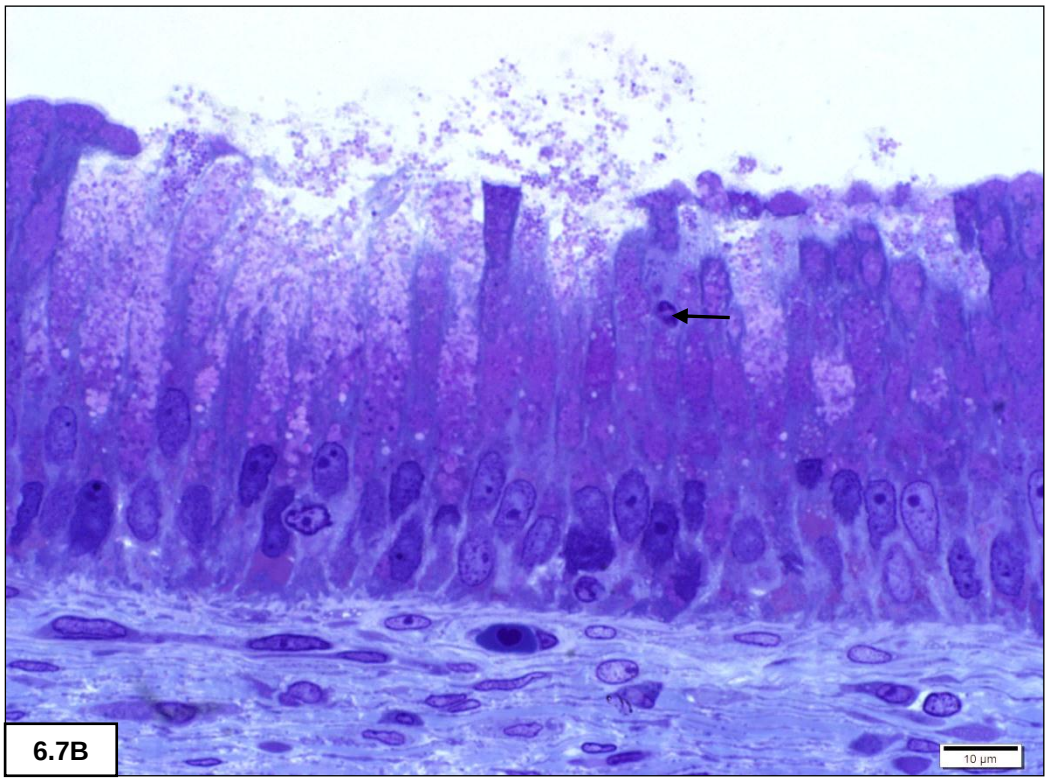

Figure 6.7B: Exocytosis of secretory granules from the epithelium. Note the pink cytoplasmic metachromasia indicating the presence of mucus and glycogen and a lymphocyte (arrow) traversing the epithelium. TB

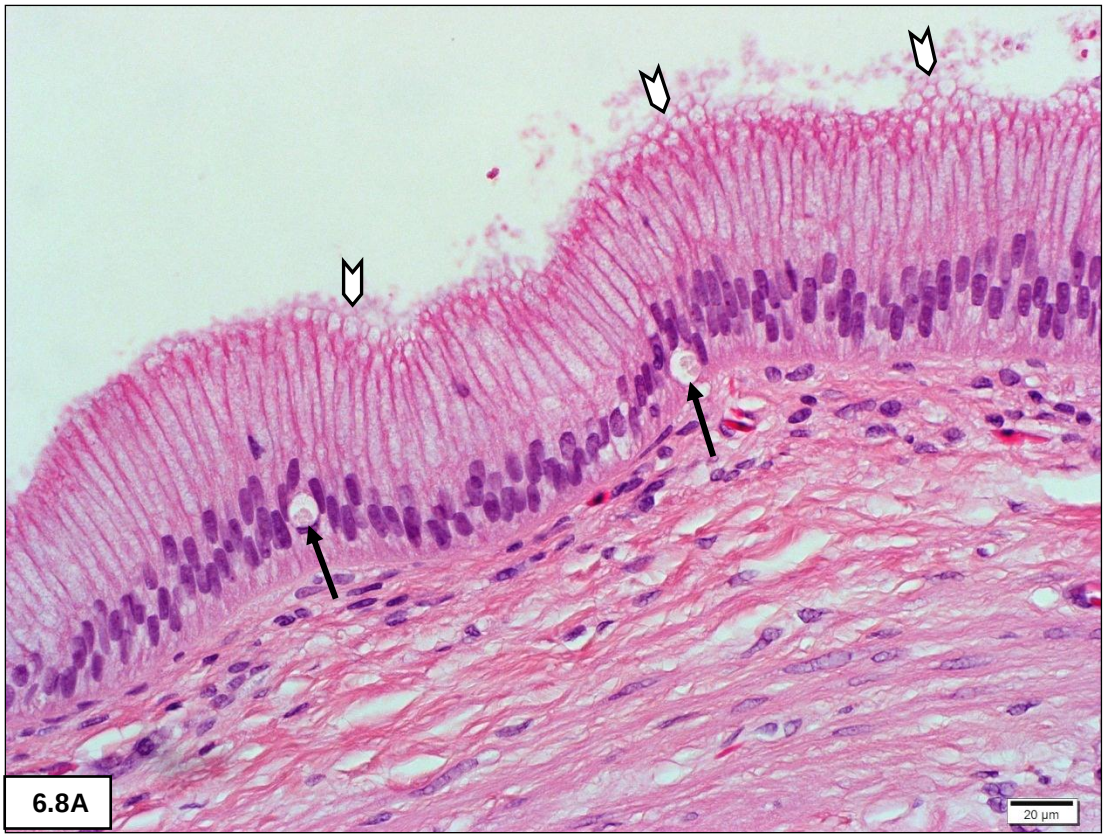

Figure 6.8: A - Vacuoles (black arrows) and apical bulging (white arrows) in the pseudostratified epithelium. H/E. **B -** Apical bulging (white arrows). TB.

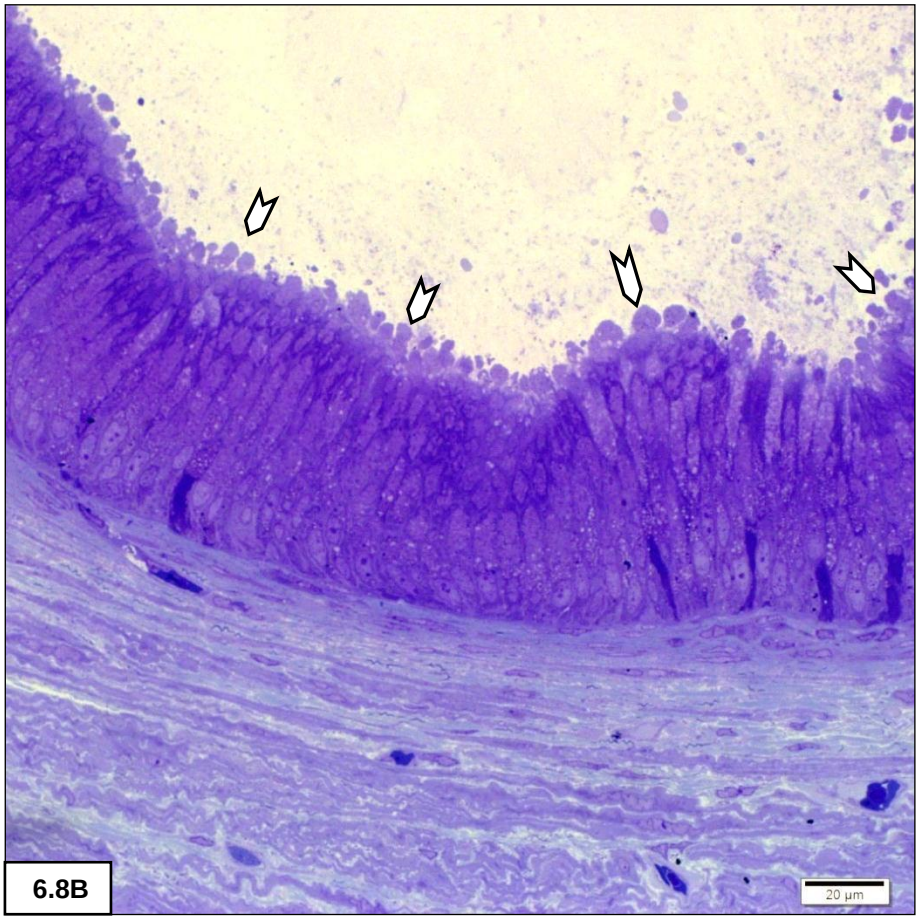

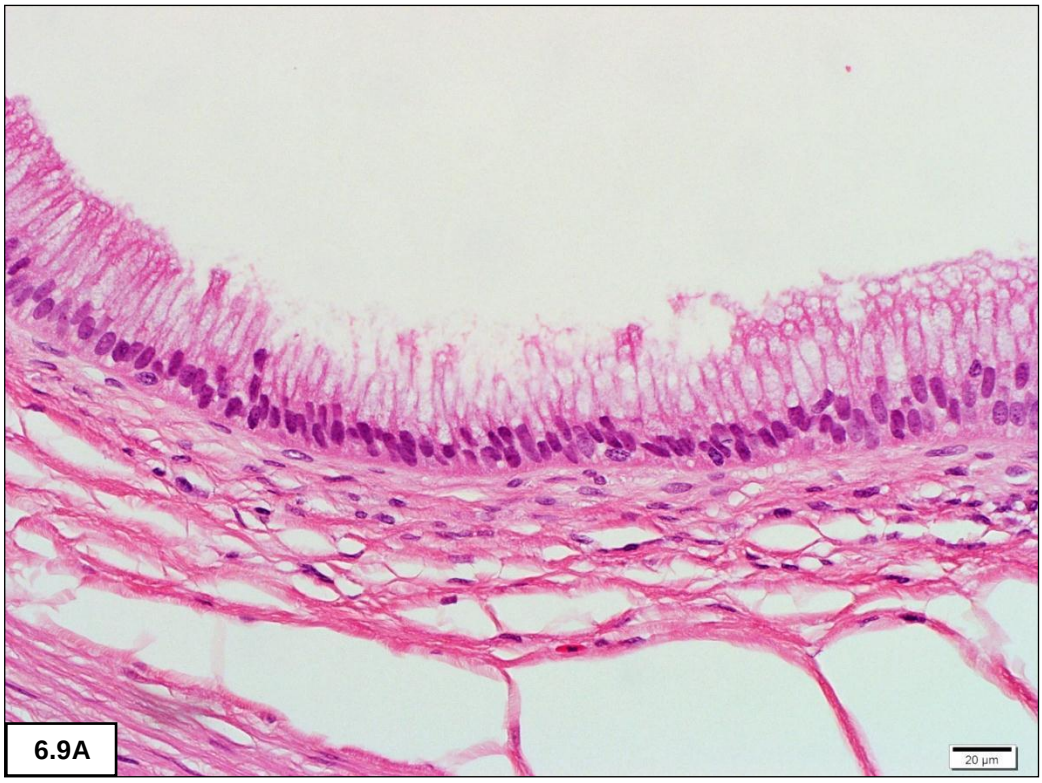

Figure 6.9A: Loss of apical portions of epithelial cells. H/E.

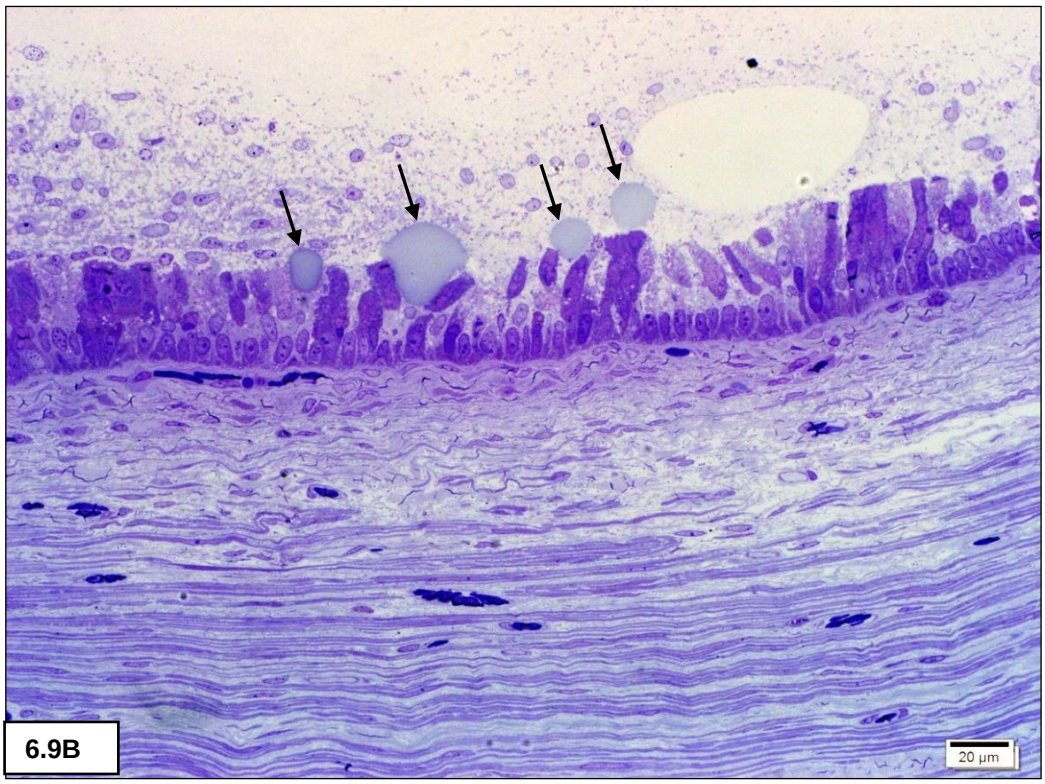

Figure 6.9B: Large lipid-like globules (arrows) attached to or near epithelial cells. Loss of cellular material from the epithelium is evidenced by the presence of cellular remnants and secretory product in the lumen. The basal nuclei are intact. The parallel arrangement of smooth muscle cells in the muscularis layer is prominent in the lower part of the image. TB.

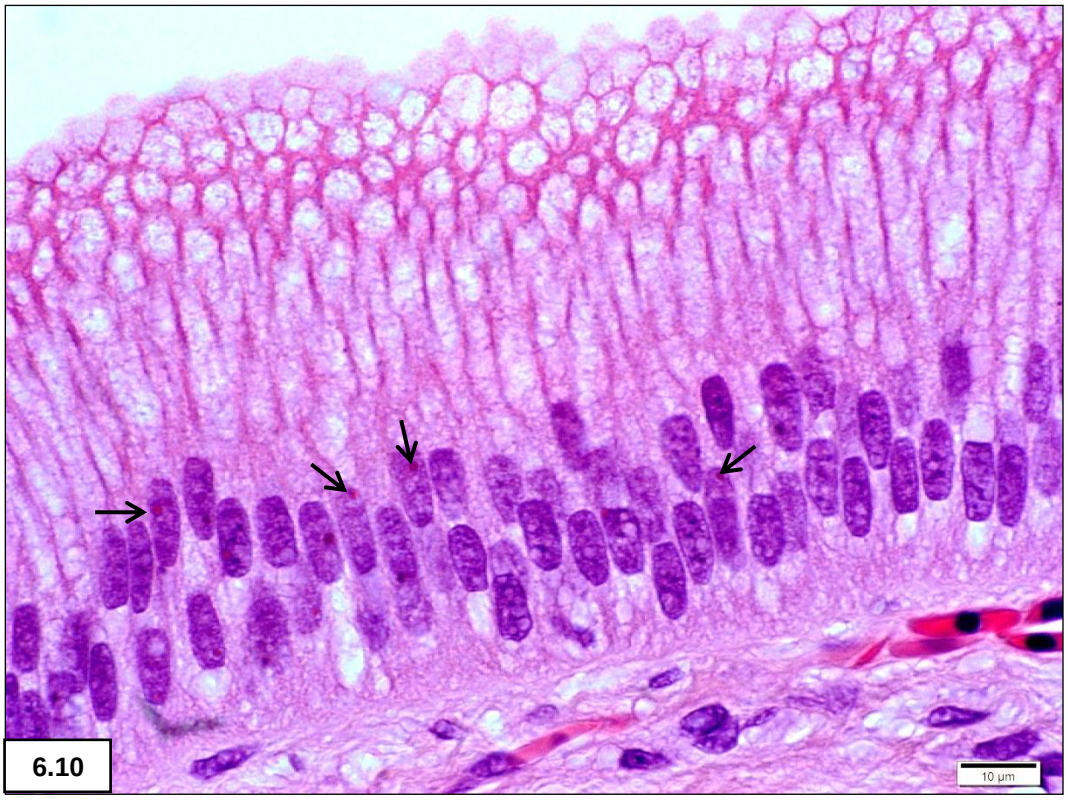

Figure 6.10: Prominent red nucleoli (arrows) in epithelial nuclei. Note different levels of nuclei typical of pseudostrtified columnar epithelium. H/E.

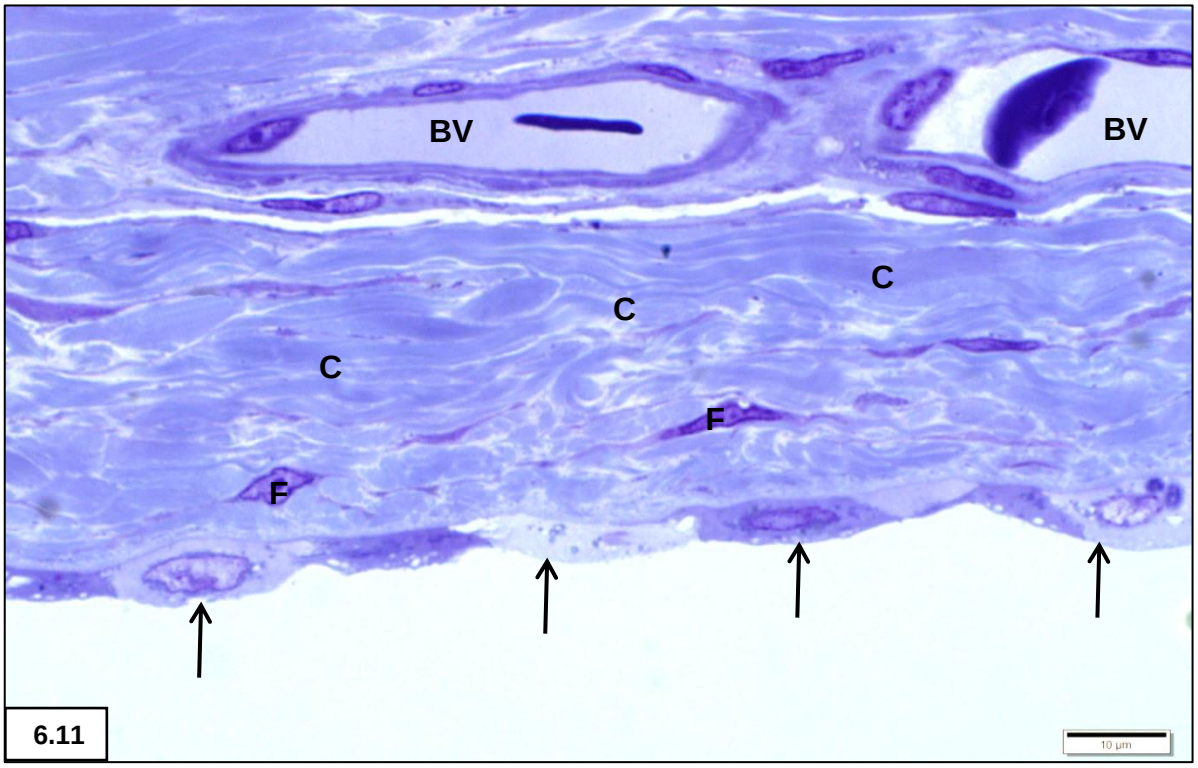

Figure 6.11: Serosa: External single layer mesothelium (arrows) covering the gallbladder with underlying subserosa consisting of supporting connective tissue, namely, collagen (**C**), fibroblasts (**F**) and blood vessels (**BV**). Note dark and light mesothelial cells. TB.

TRANSMISSION ELECTRON MICROSCOPY: PSEUDOSTRATIFIED EPITHELIUM

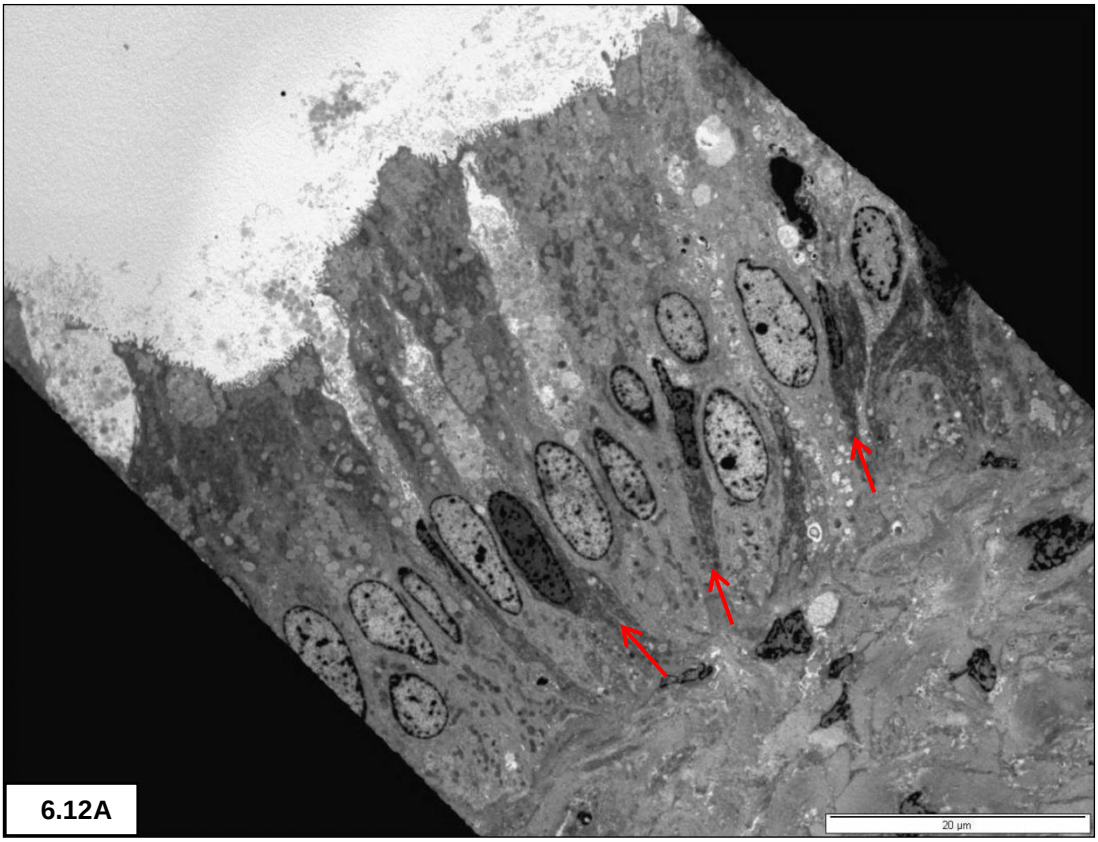

Figure 6.12 A & B: Pseudostratified columnar epithelium with slender dark cells (red arrows) interposed between light cells. Note lymphocyte (yellow arrow) in **B**.

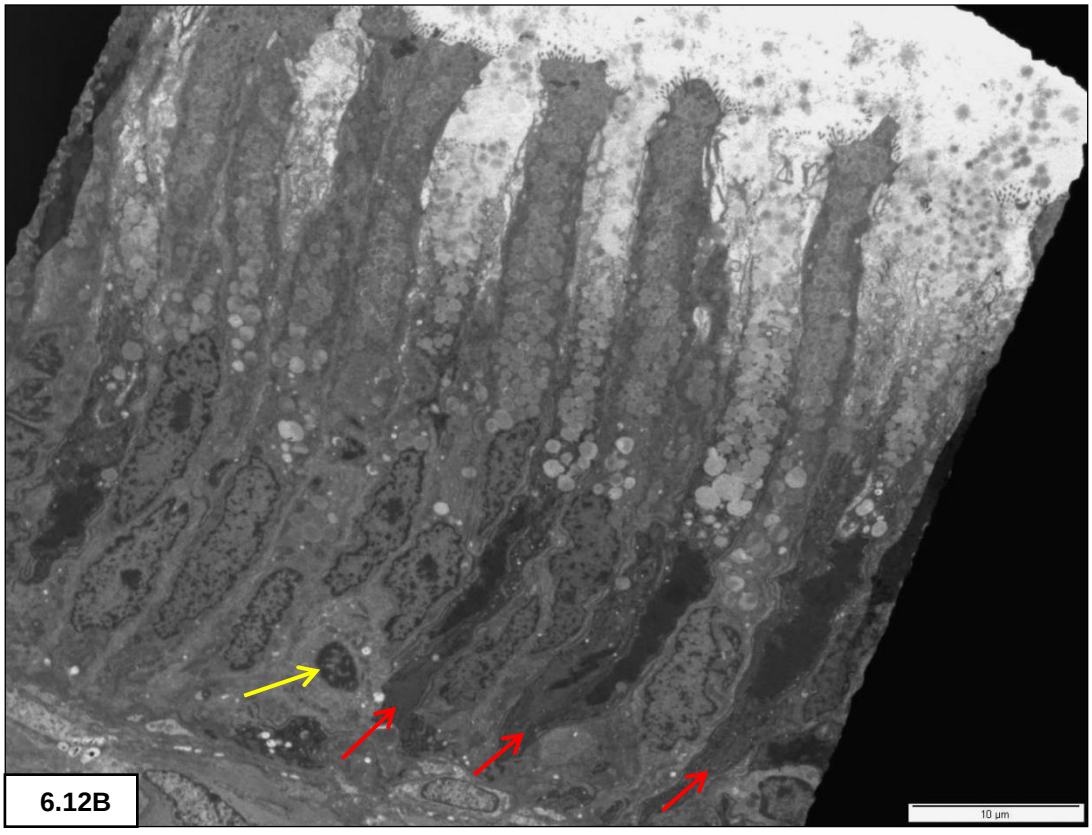

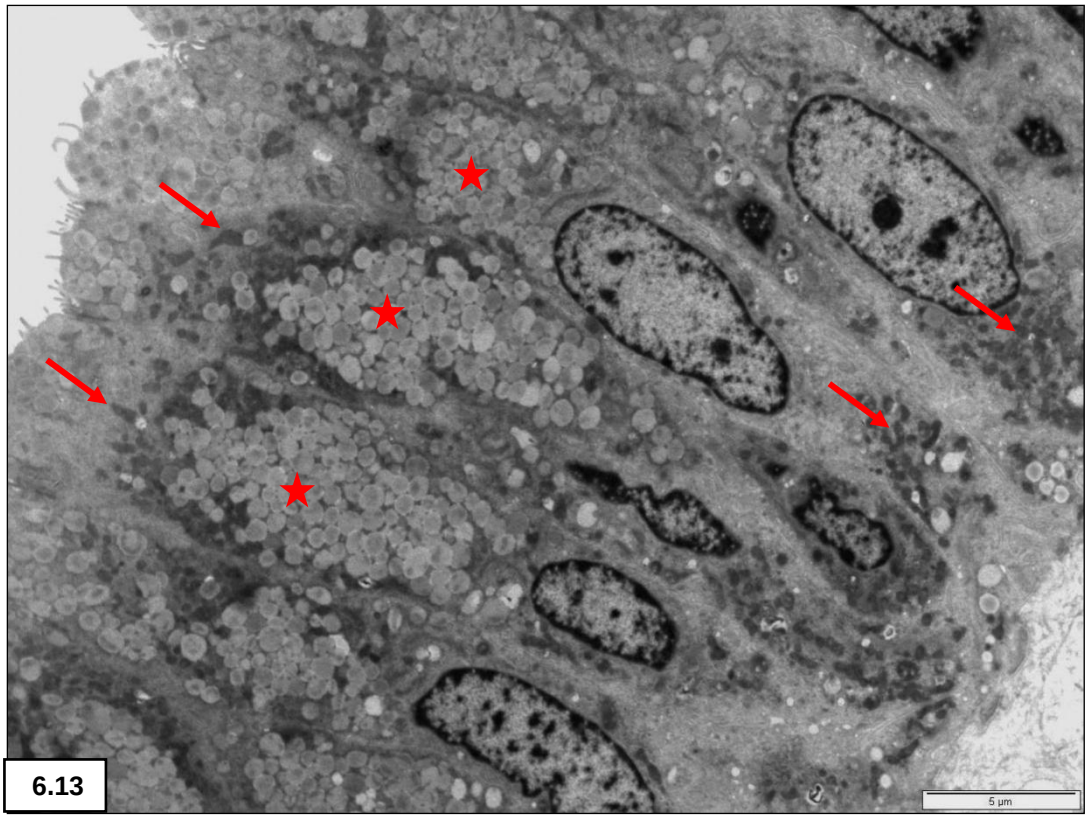

Figure 6.13: Slender goblet cells packed with secretory granules (stars). Note concentrations of basal & apical mitochondria (arrows) and oval-shaped nuclei.

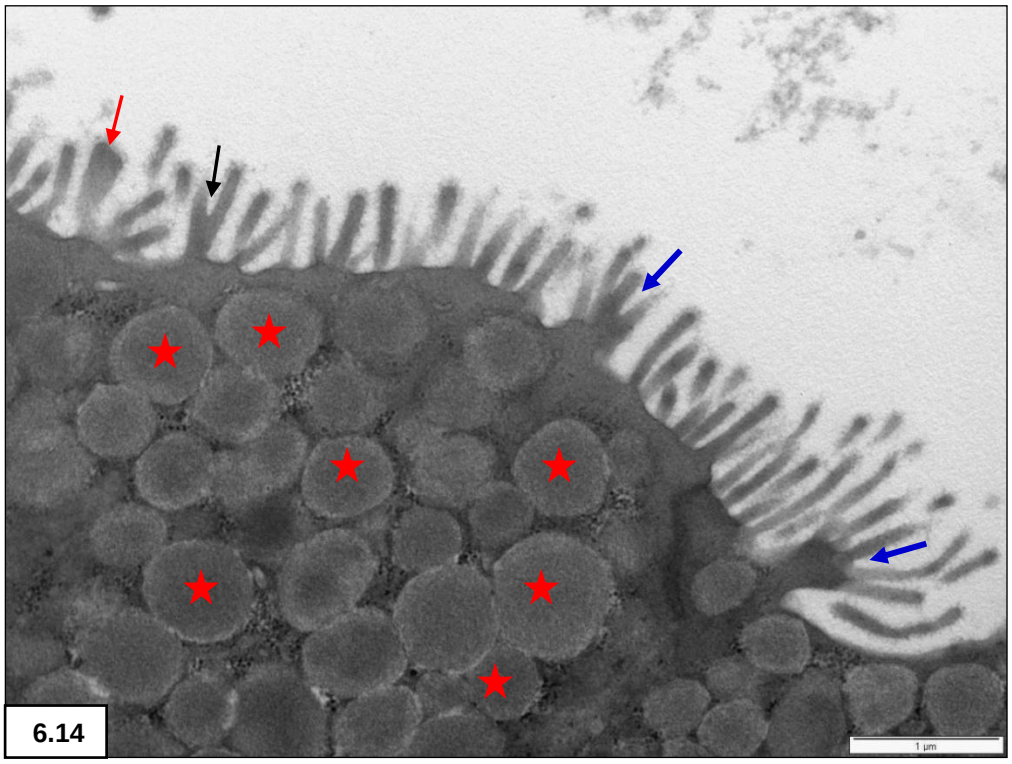

Figure 6.14: Staghorn (black arrow), branching (blue arrows) and club-shaped (red arrow) microvilli on apices. Note glycocalyx covering the villi. Spherical secretory granules of medium electron density (stars).

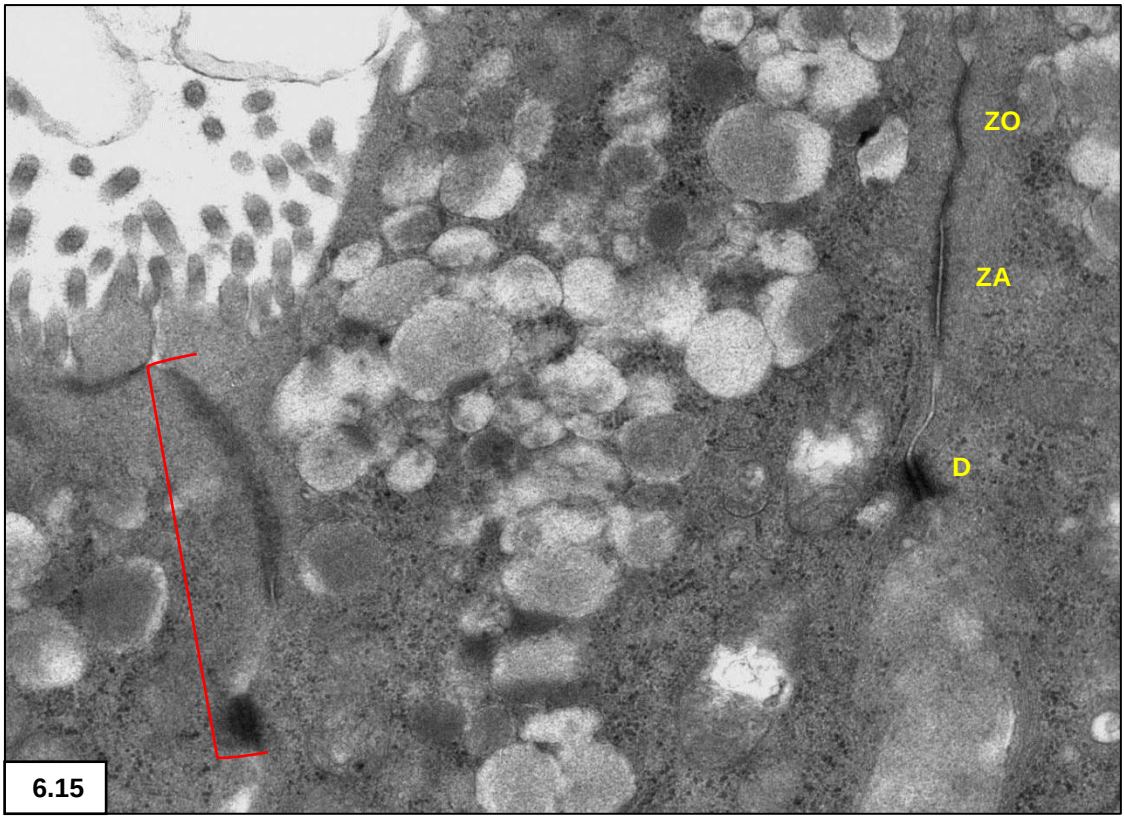

Figure 6.15: Apical junctional complex composed of a zonula occludens (ZO), zonula adherens (ZA) and desmosome (D). A second junctional complex (bracket) is sectioned obliquely.

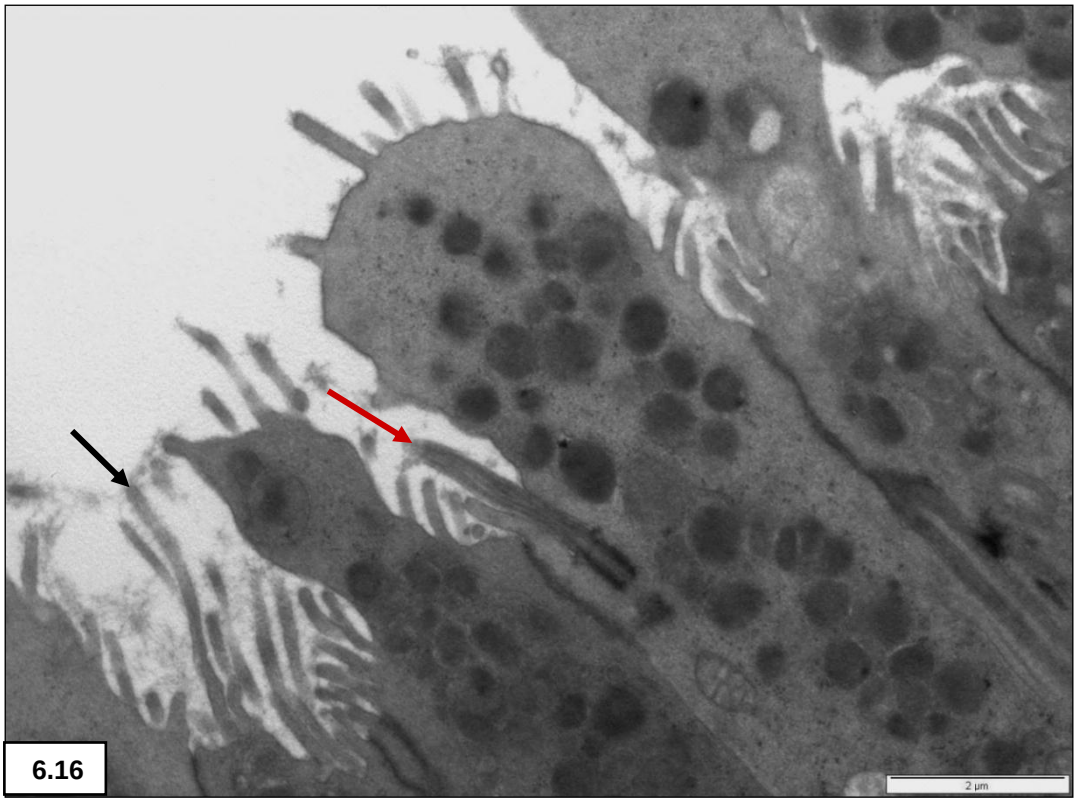

Figure 6.16: A cilium protruding from the cell apex (red arrow). Note bulging apices and a single long microvillus (black arrow).

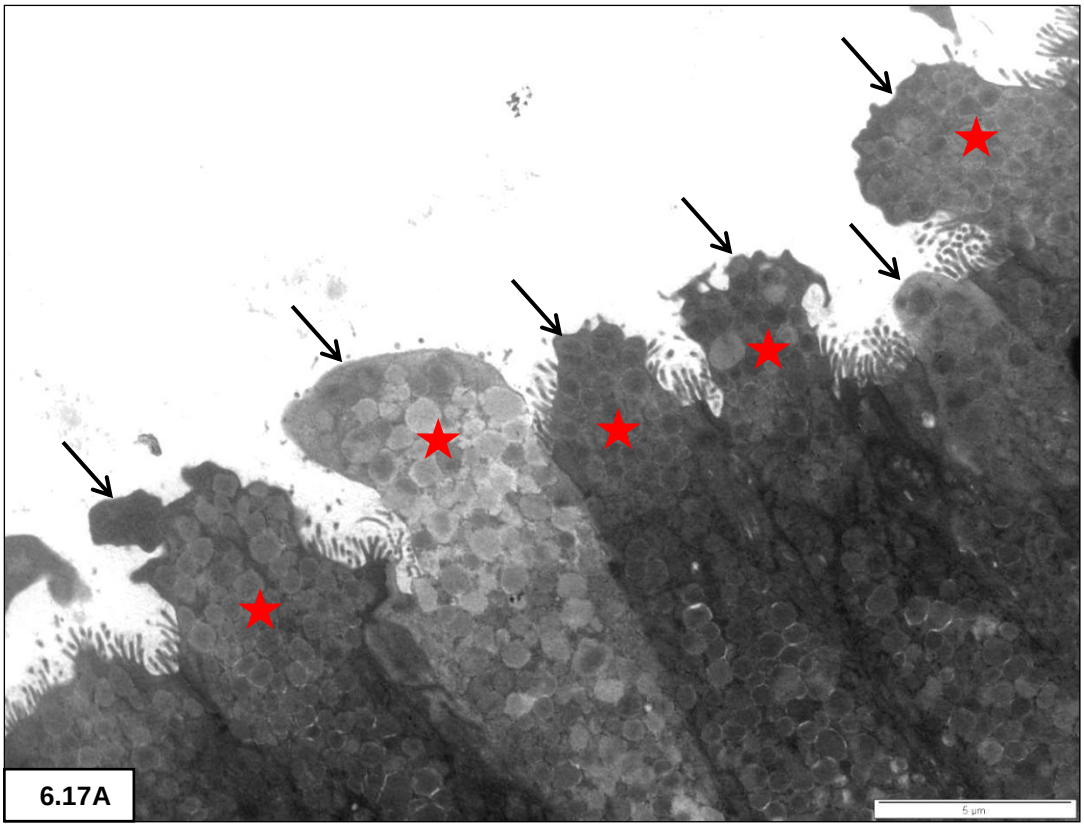

Figure 6.17: A & B: Collections of secretory granules (stars) in the subapical space and apical bulging with decrease or loss of microvilli (black arrows). **B:** Note junctional complexes (red arrows) and the fusion of granules forming vacuoles (blue arrow).

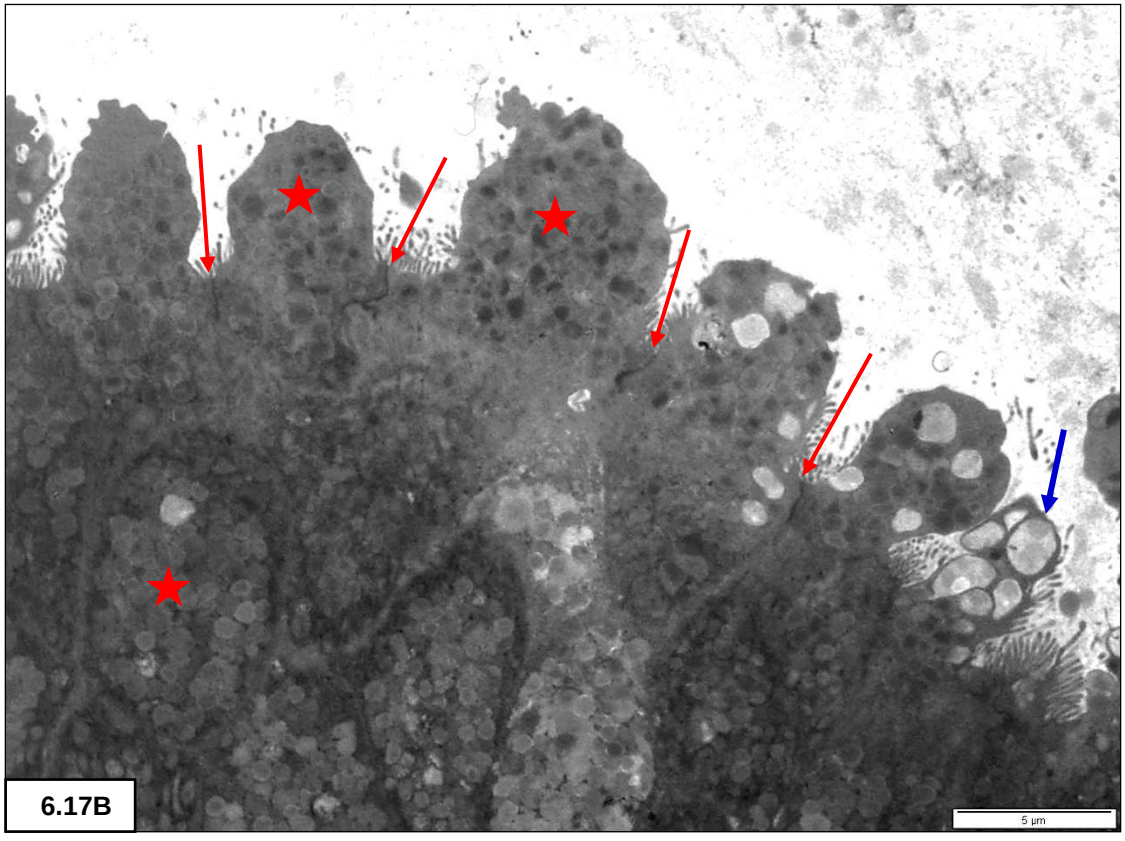

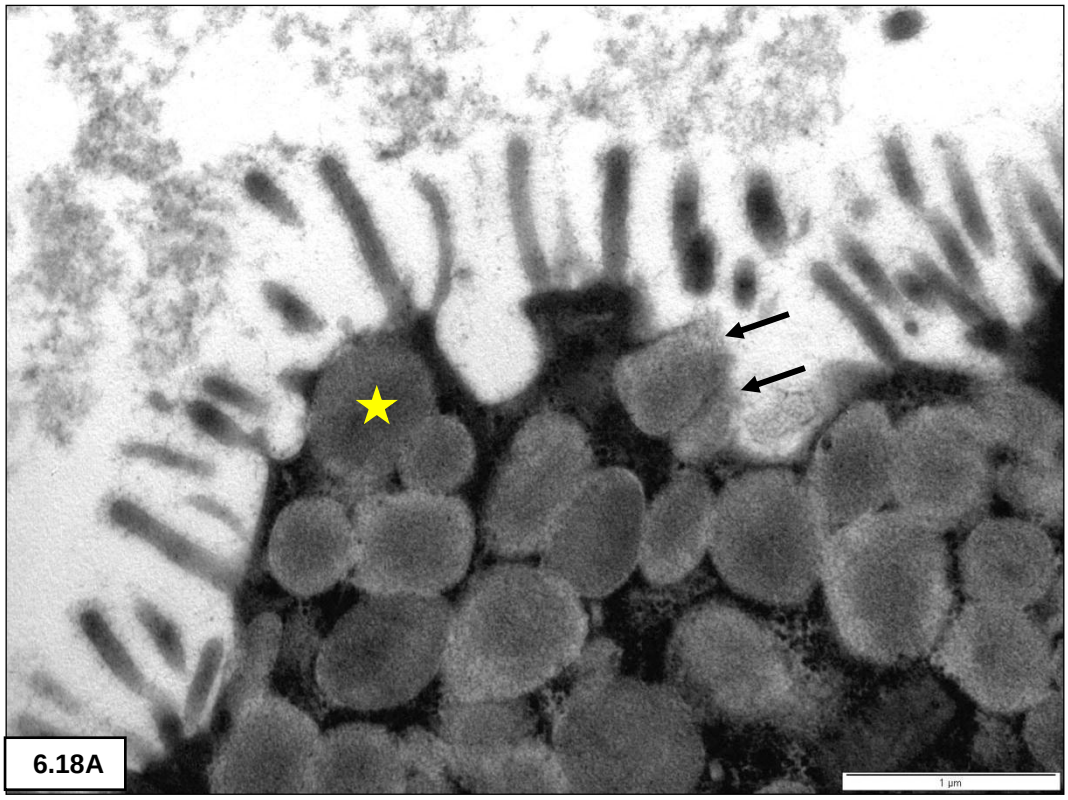

Figure 6.18: A: Exocytosis of secretory granules (black arrows). Note granule at the point of merging with the cell membrane (star).
B: Goblet cell at the point of extruding secretory granules (red arrow).Note junctional complex (bracket).

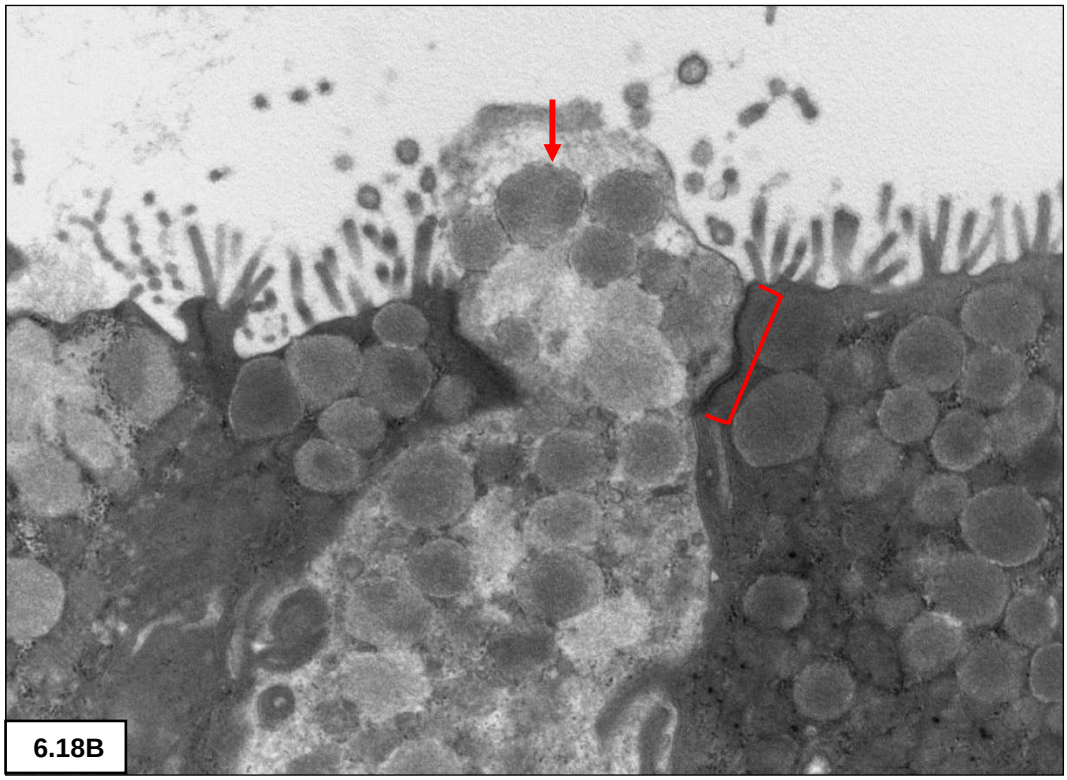

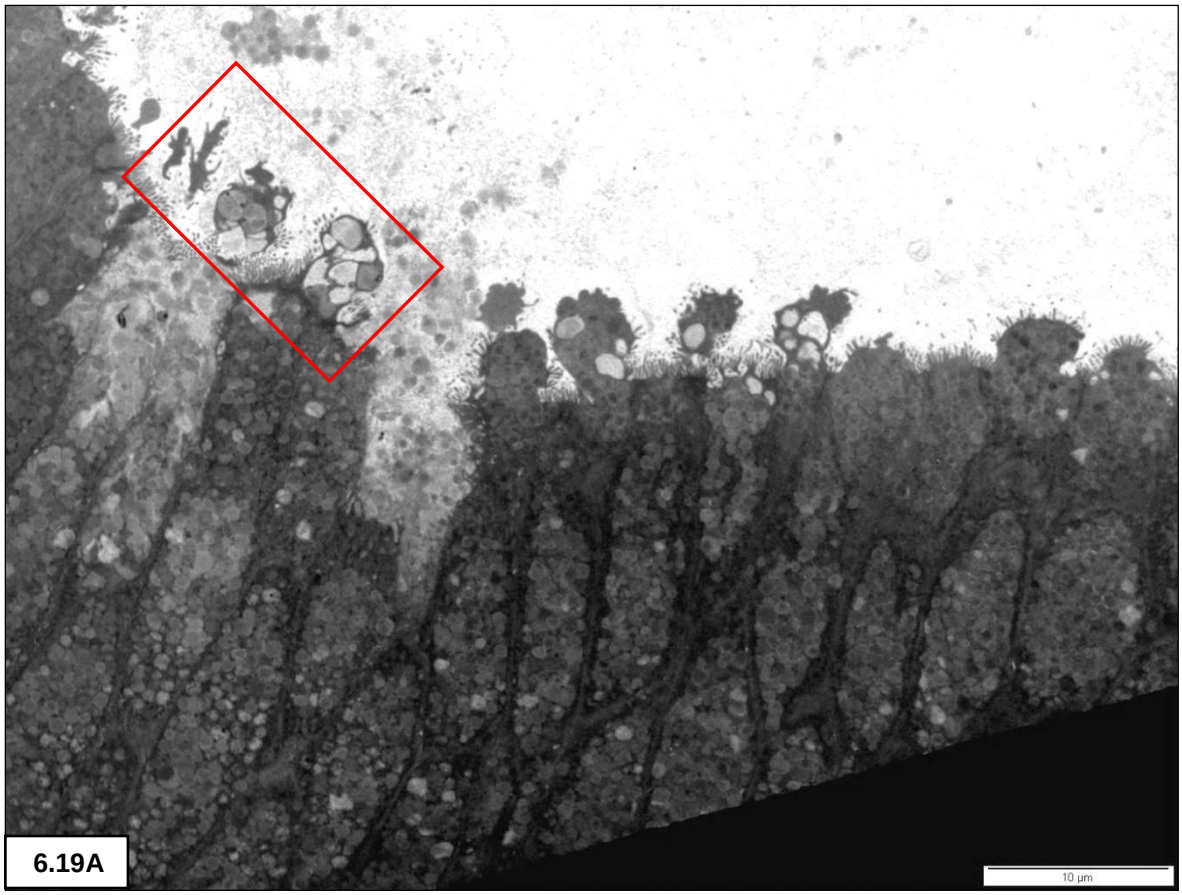

Figure 6.19: A: Different stages of apical bulging.
B: Blocked area in A - Pinching off of apical cell cytoplasm.

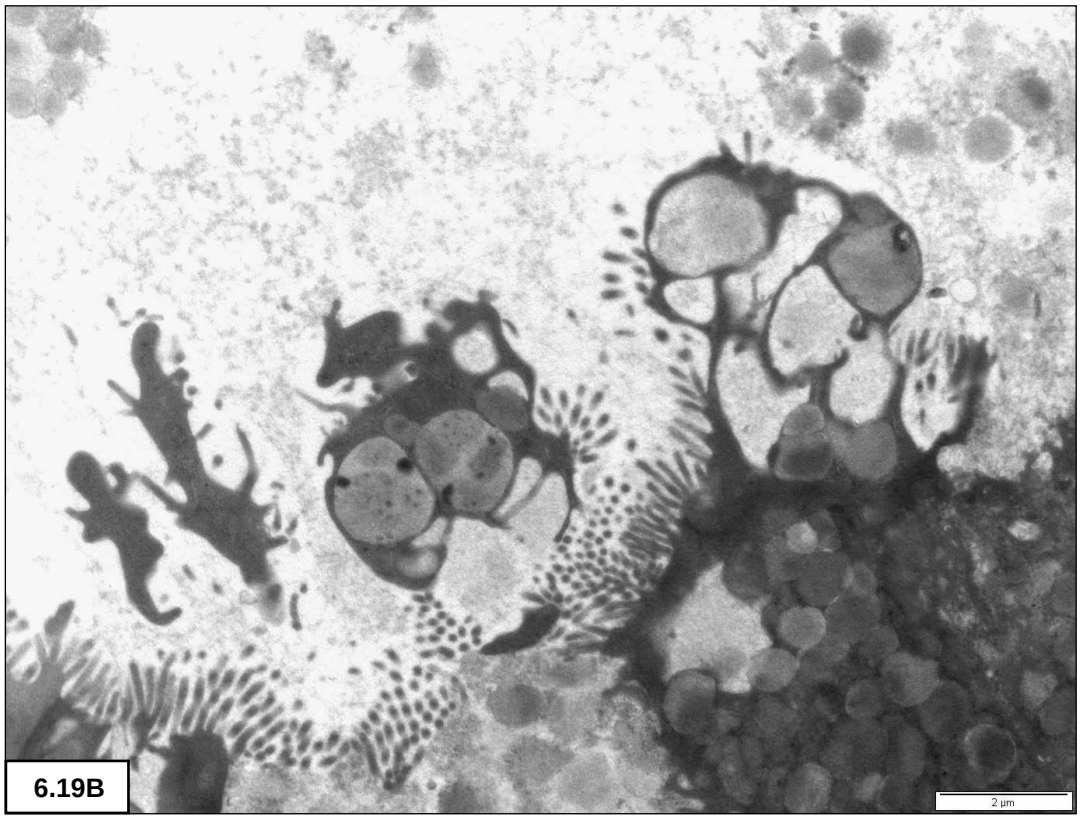

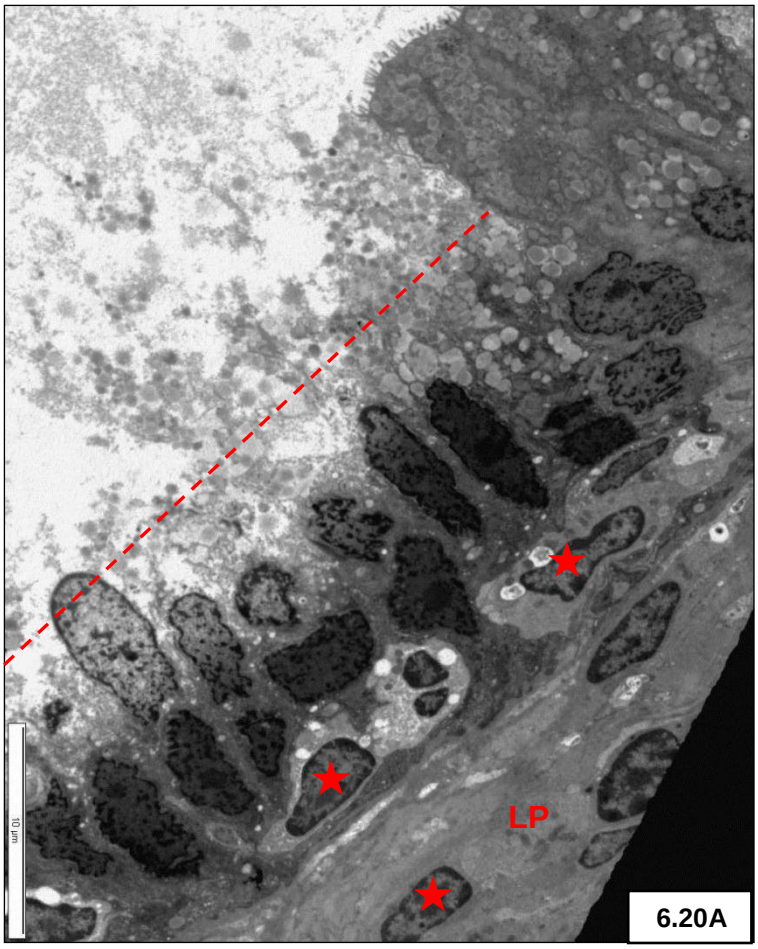

Figure 6.20: A & B: Loss of cell apices (dashed line in **A**) with an increase of dark cells with corrugated nuclei. Note lymphocytes (stars) positioned at the base of the epithelium and in the lamina propria (LP) just beneath the basal lamina.

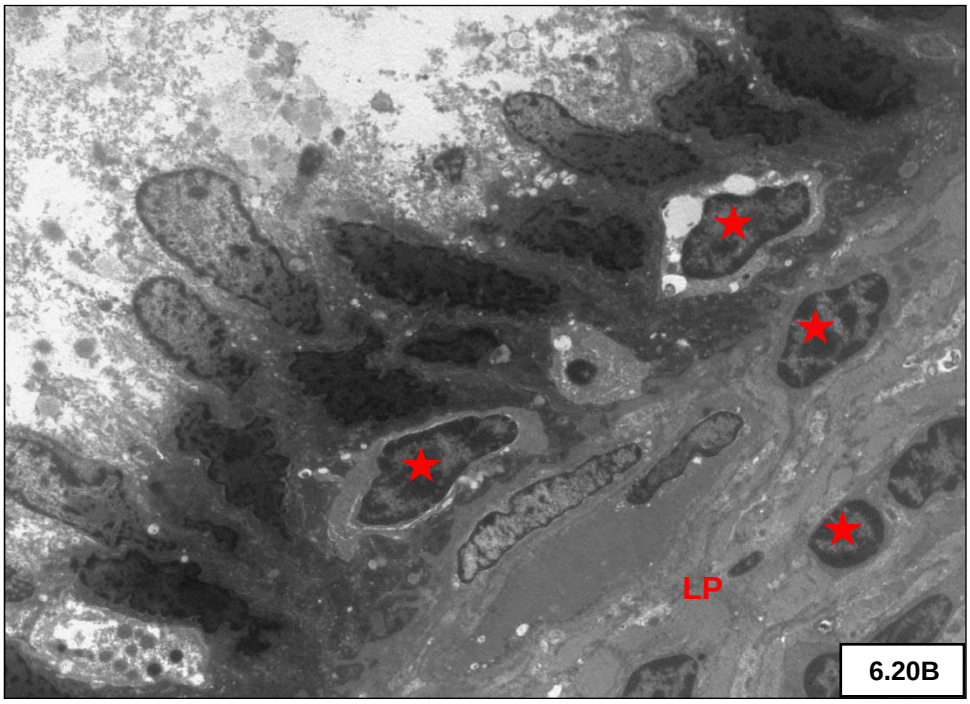

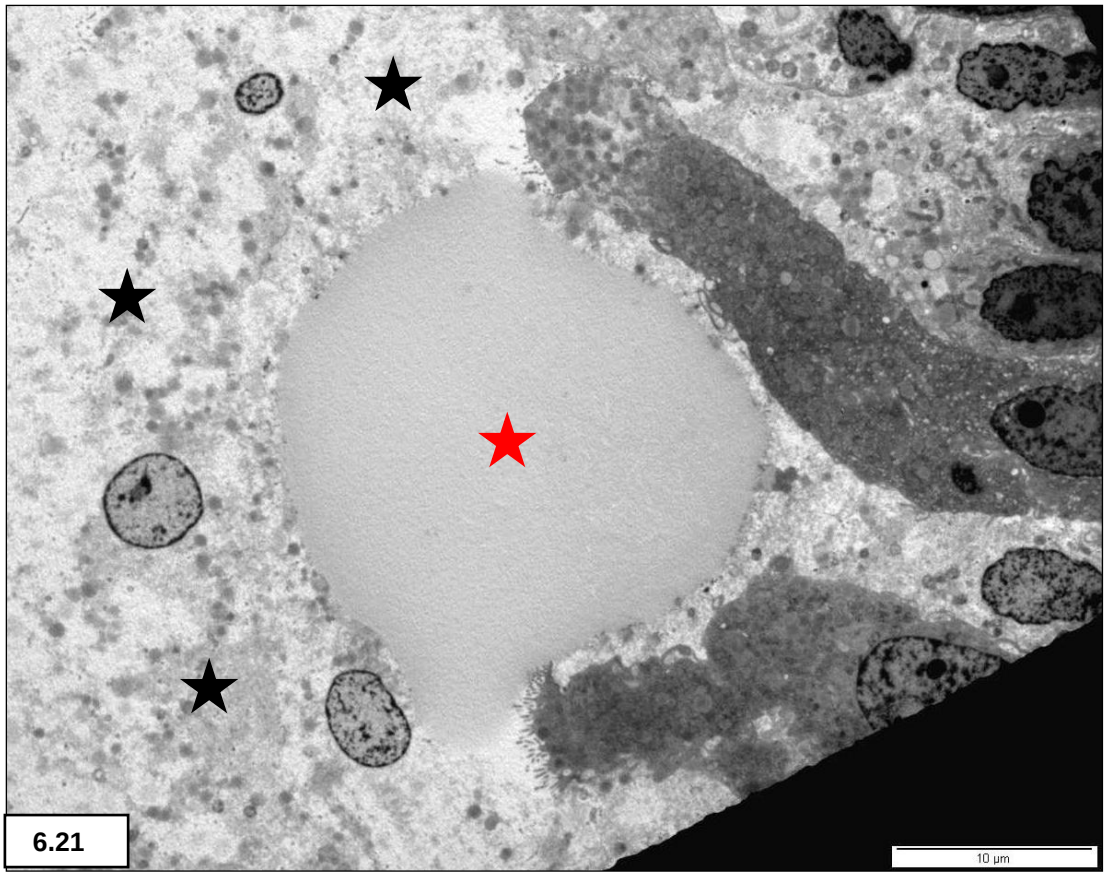

Figure 6.21: Lipid-like globule (red star) closely associated with the surface epithelium. Note cell debris in the lumen (black stars).

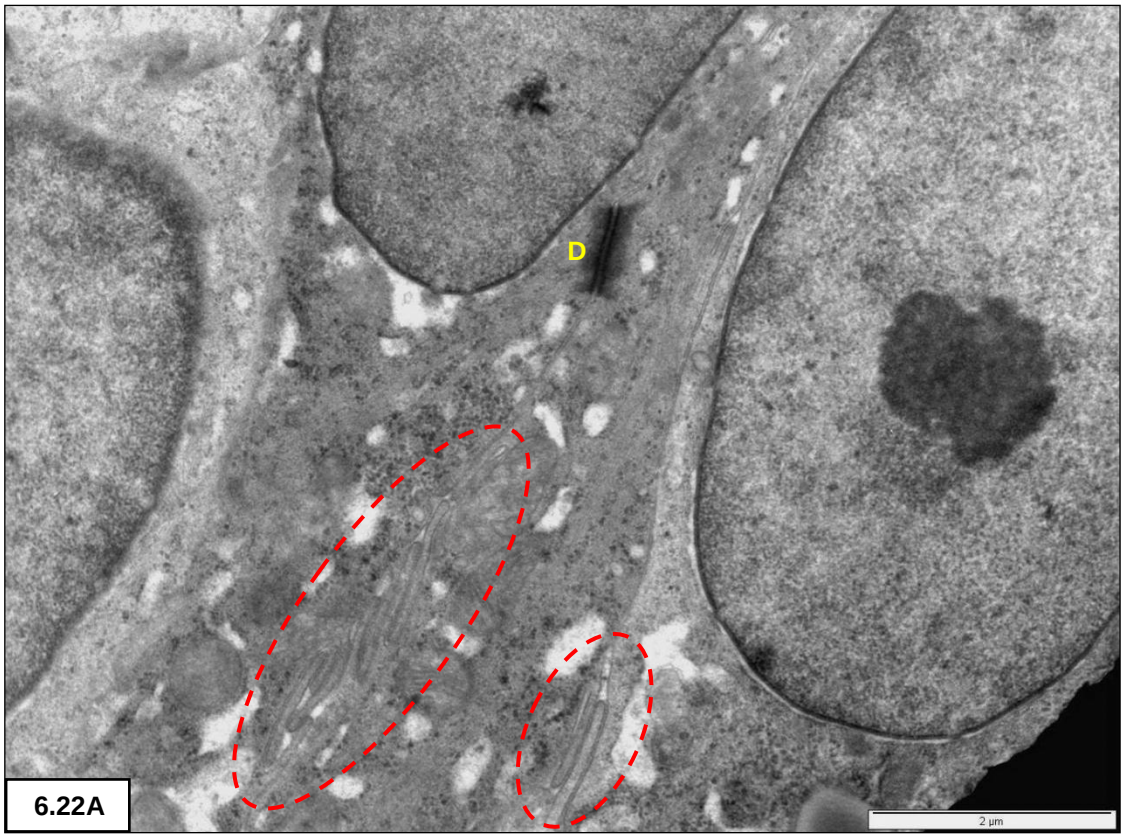

Figure 6.22: A - Desmosome (D) between lateral cell borders. **A & B**: Note lateral interdigitations of the cell membranes (dashed lines). **B –** Golgi apparatus (yellow arrow), granular endoplasmic reticulum (red arrows).

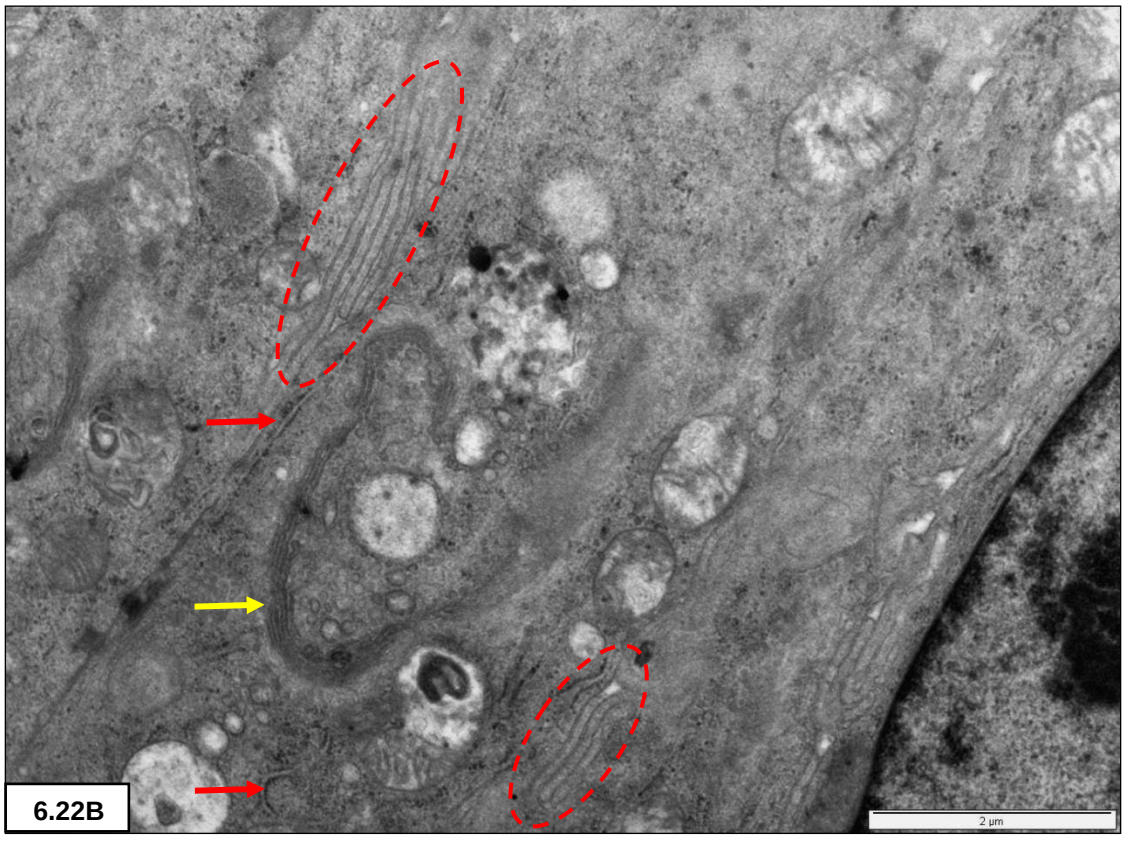

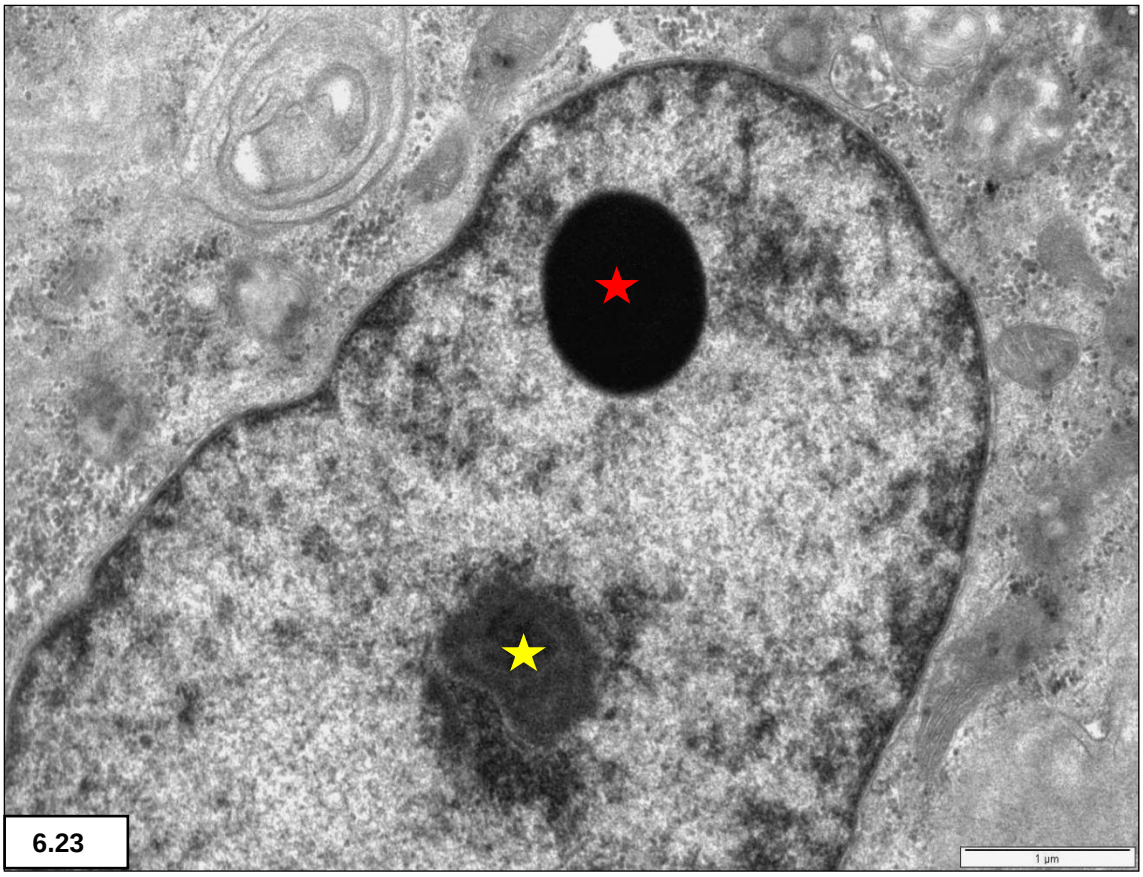

Figure 6.23: Two nucleoli – note the prominent circular electron-dense nucleolus (red star) and the more typical amorphous nucleolus (yellow star).

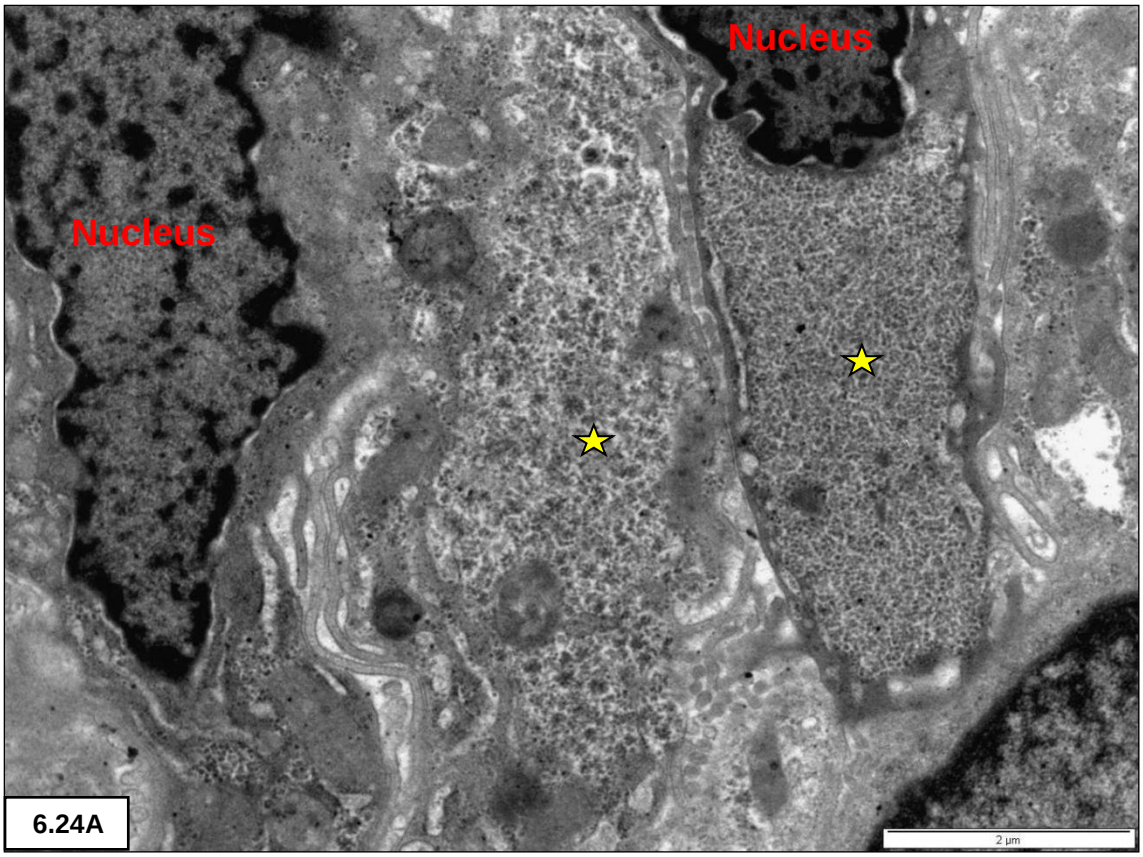

Figure 6.24 A: Collections of glycogen granules (stars) at the base of adjacent cells.
B: Intermediate filaments (yellow arrows), mitochondria (red arrows).

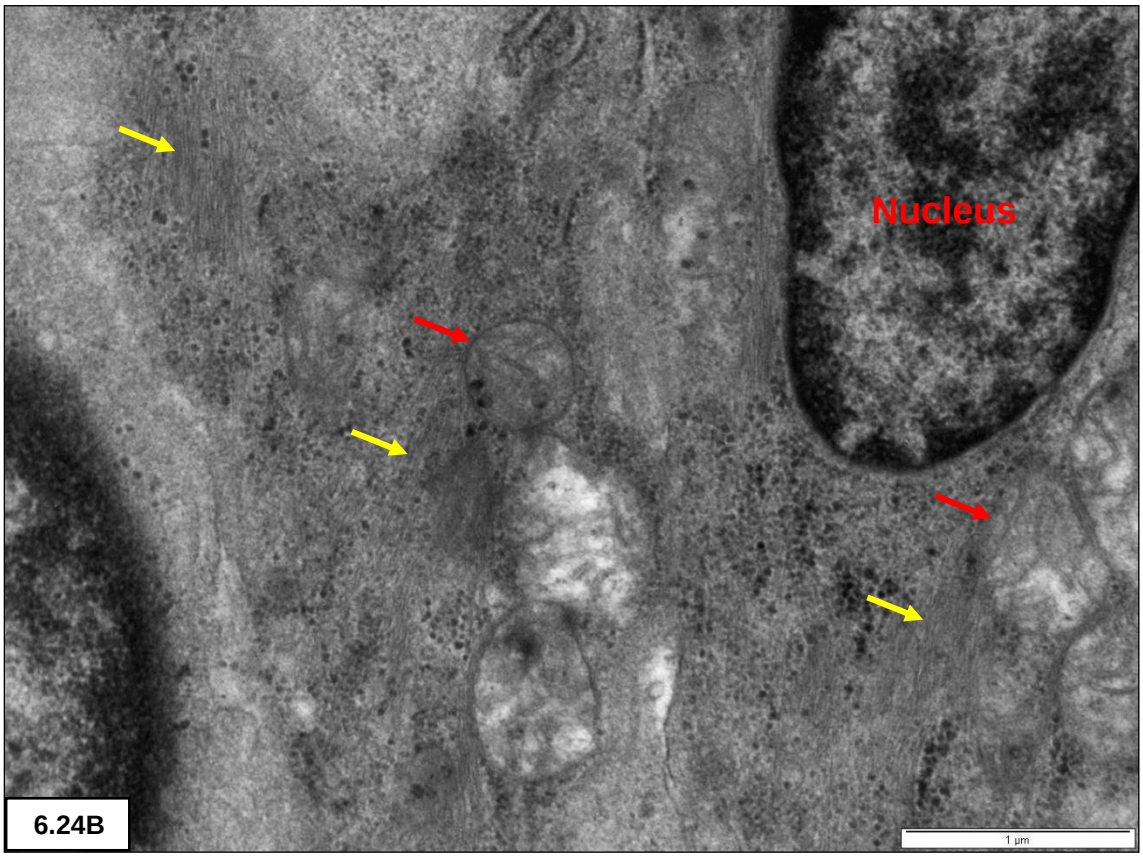

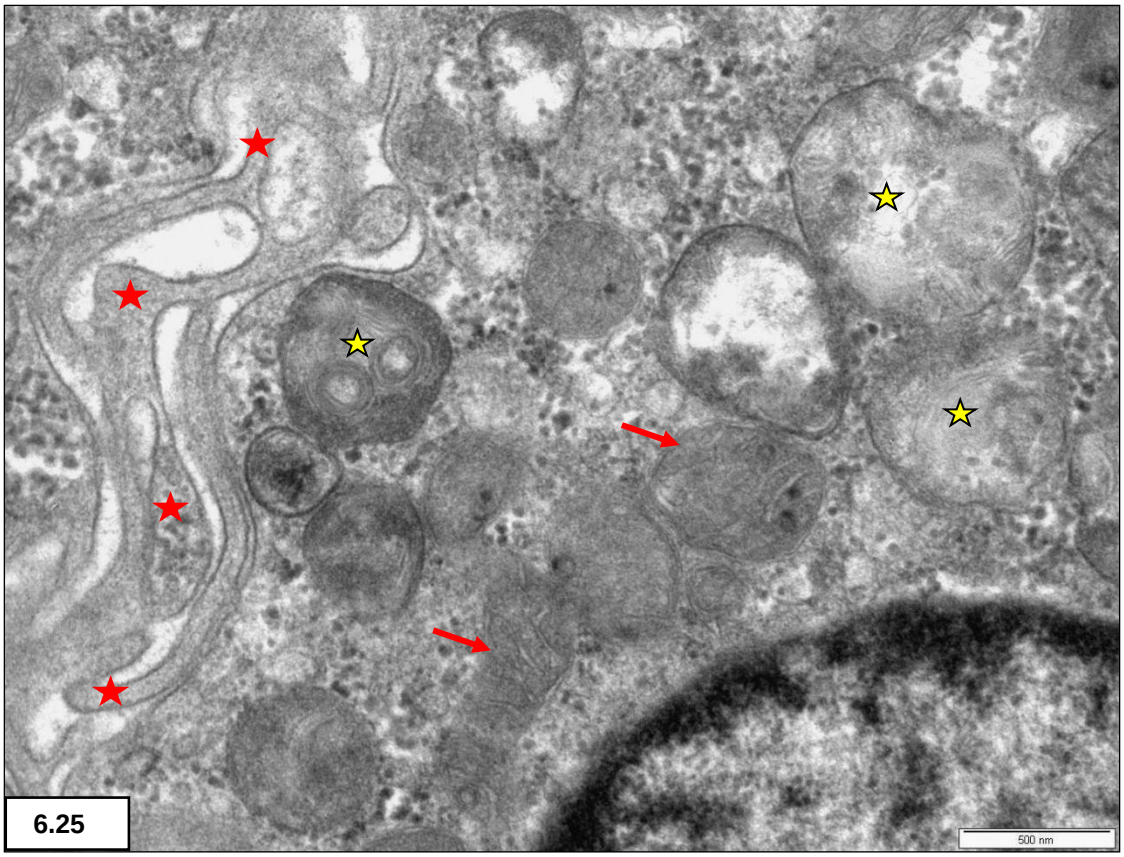

Figure 6.25: Lysosomes with whorled membranes (yellow stars).
Note mitochondria (arrows) and interdigitating cell membranes (red stars).

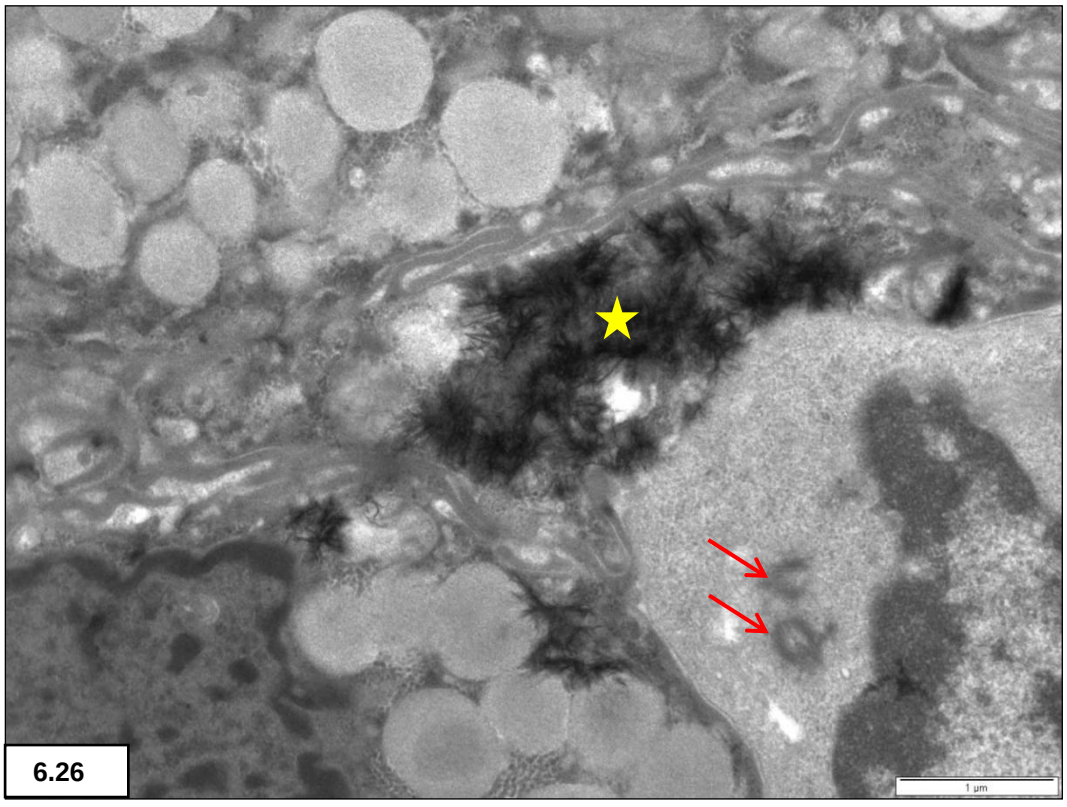

Figure 6.26: Electron-dense calcium deposits (yellow star). Note centrioles (arrows).

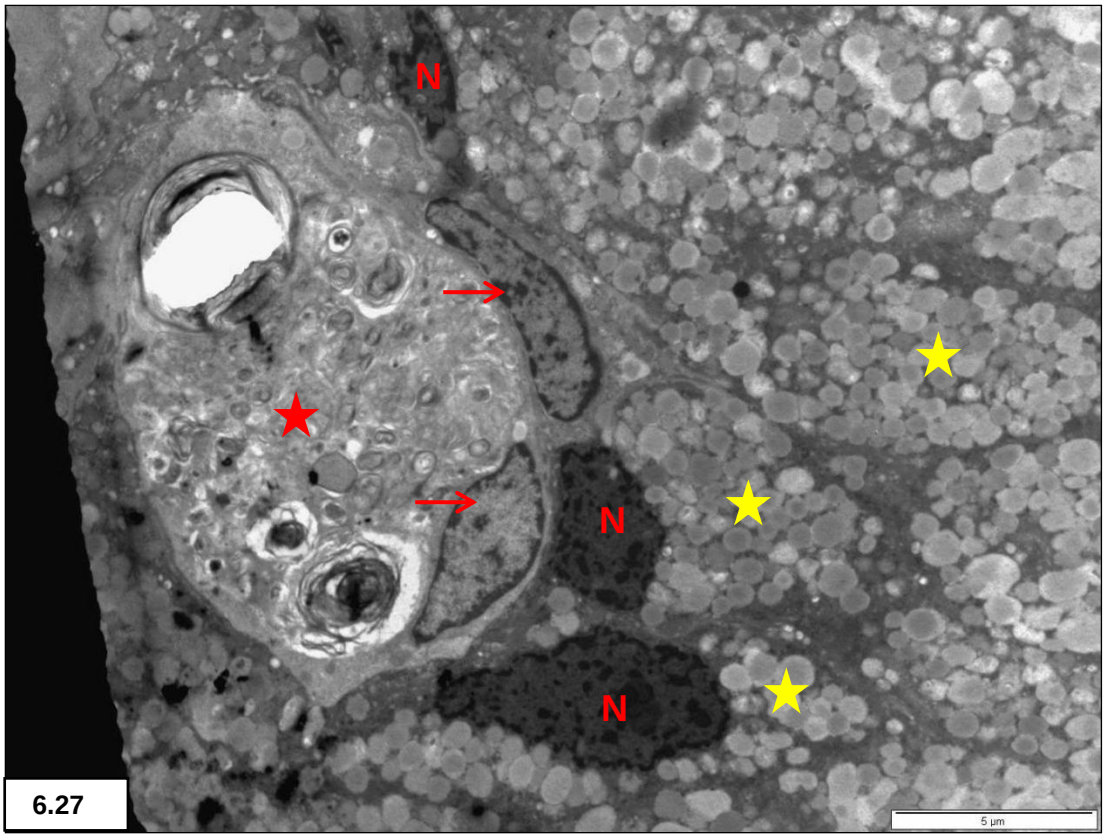

Figure 6.27: Cytoplasmic vacuoles filled with membranous debris (red star) present in macrophages between the pseudostratified columnar epithelial cells. Macrophage nuclei (arrows). Secretory granules (yellow stars) and nuclei (**N**) of epithelial cells.

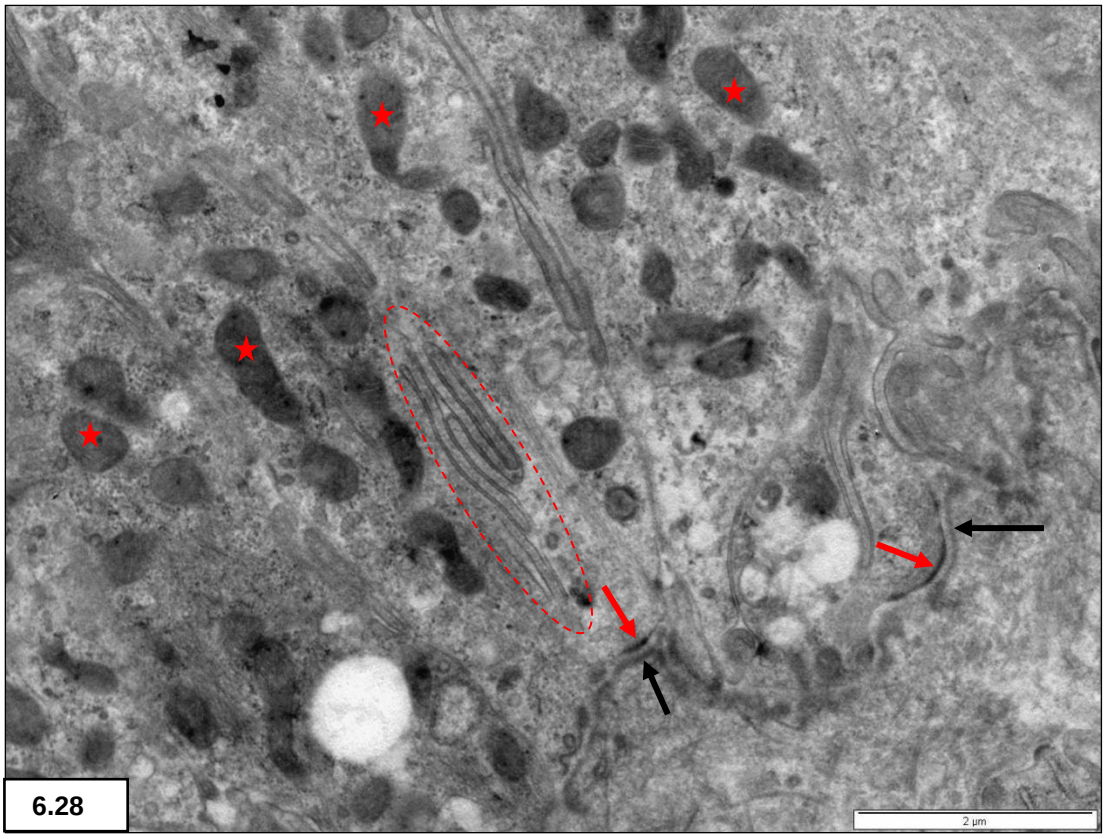

Figure 6.28: Undulating basal lamina (black arrows), hemidesmosomes (red arrows), basolateral interdigitations (dashed line). Note mitochondria (stars).

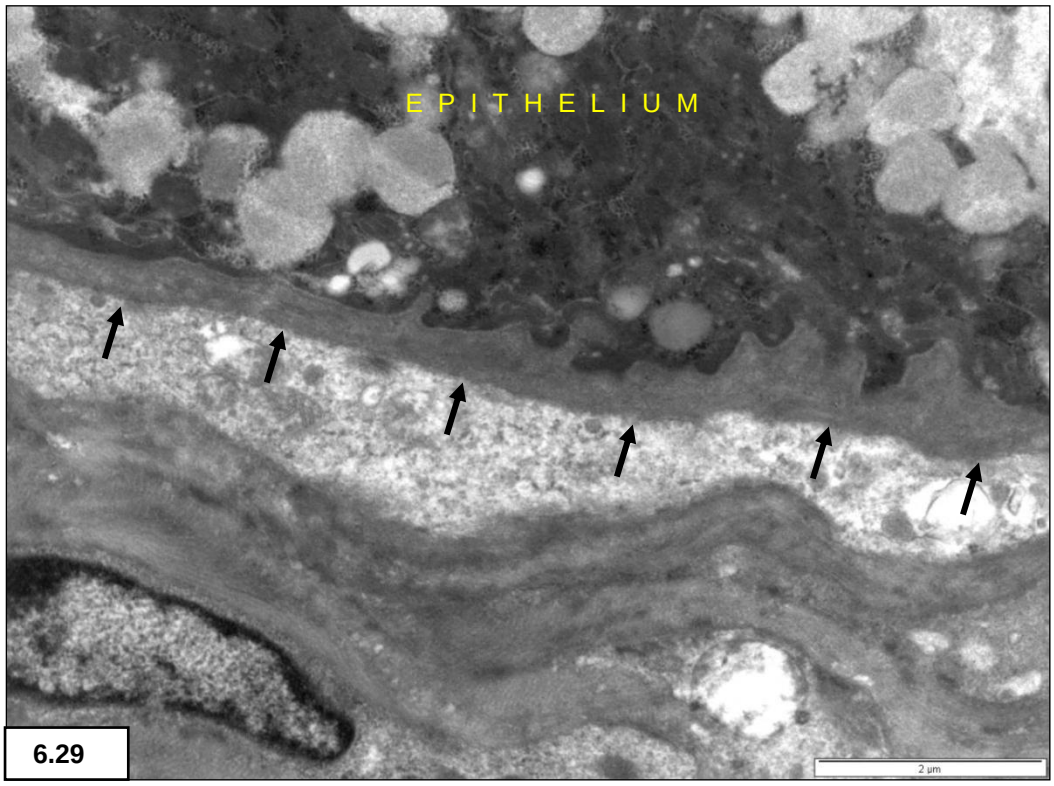

Figure 6.29: Thickened basal lamina (arrows) beneath a cell displaying apical loss of cytoplasm.

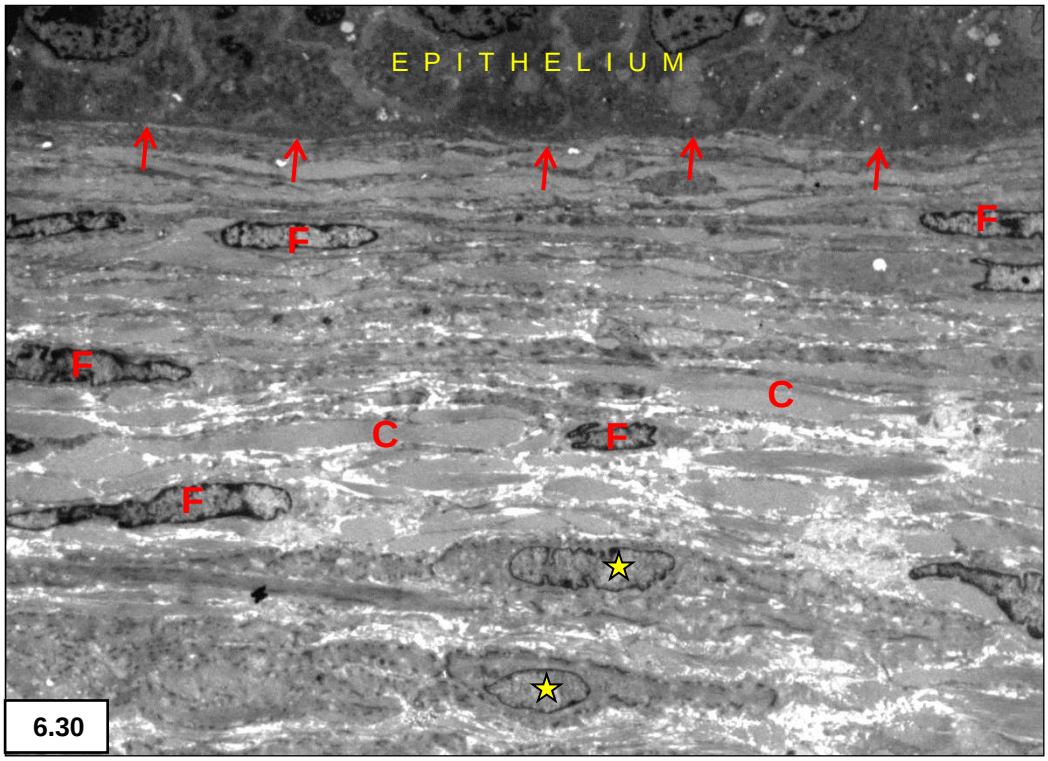

Figure 6.30: *Lamina propria* - smooth muscle cells (stars) relatively near basal lamina (arrows). Fibroblasts (**F**) with intervening collagen (**C**) also present.

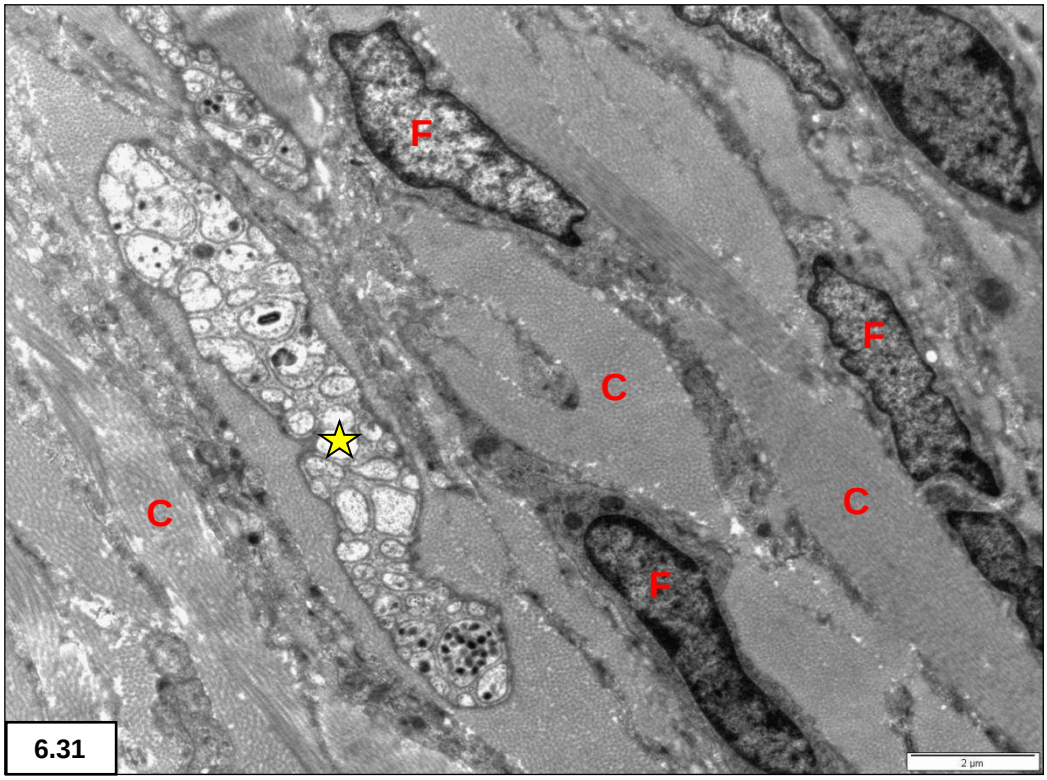

Figure 6.31: A nerve ganglion (star) among sheets of collagen fibres (**C**) and accompanying fibroblasts (**F**) in the *lamina propria.*

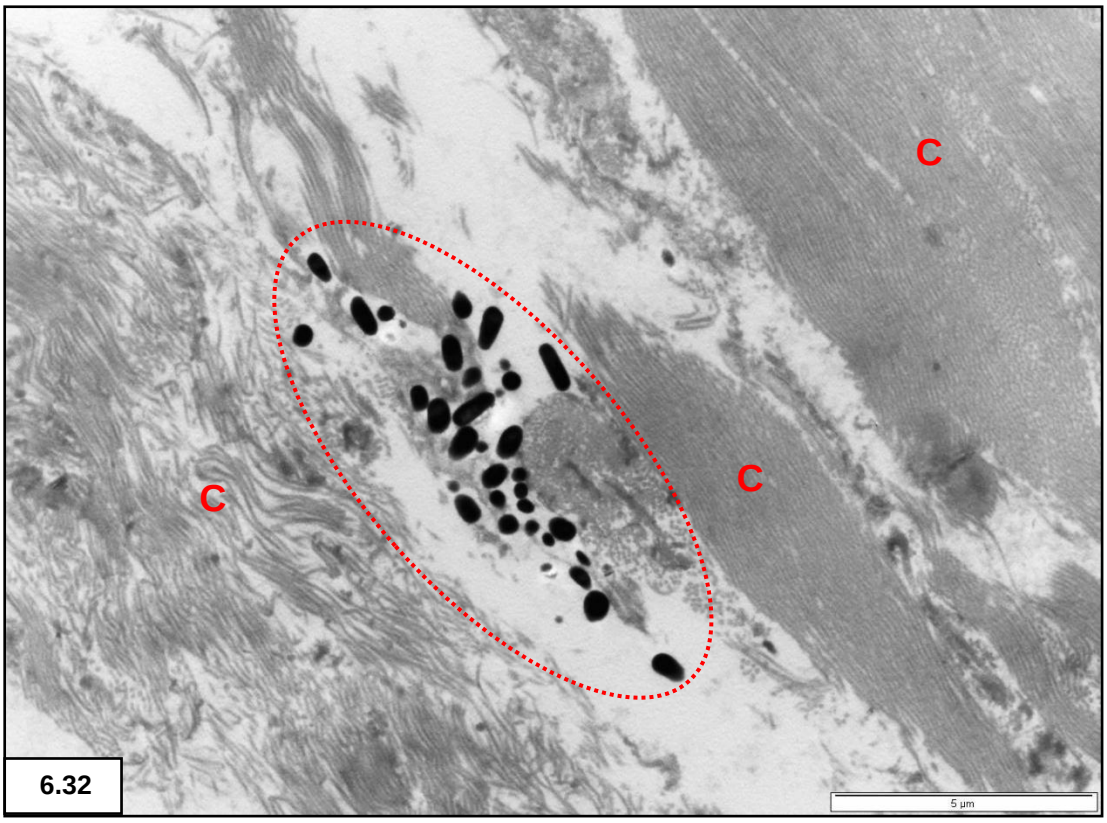

Figure 6.32: Loose lying melanin granules (dashed circle) between collagen fibres (**C**) in the *lamina propria*.

MUSCULARIS EXTERNA

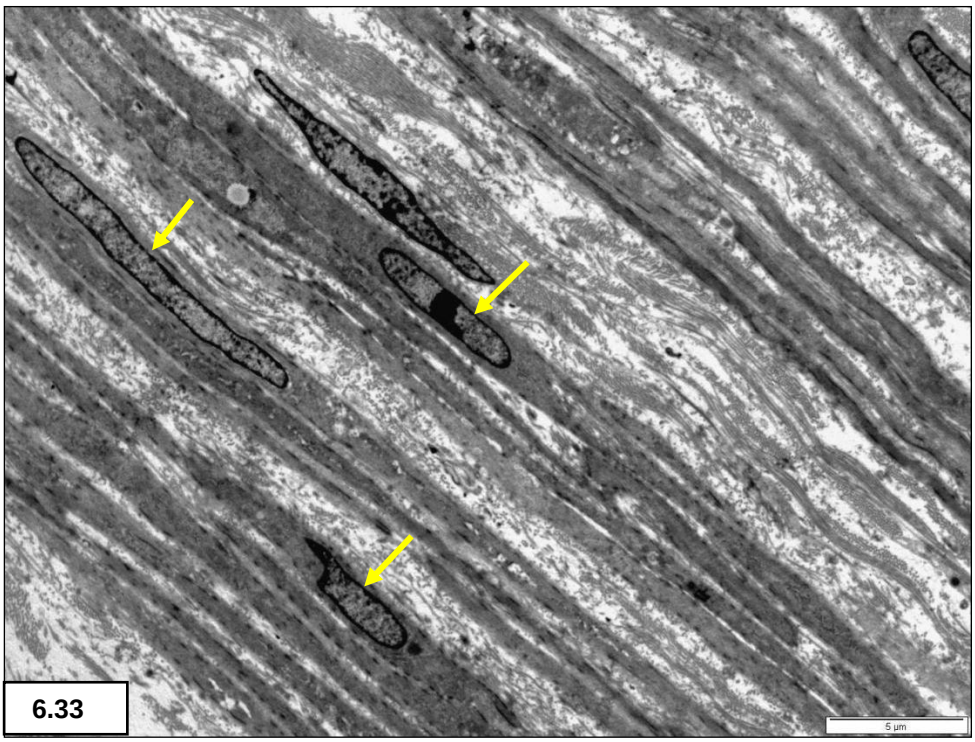

Figure 6.33: *Muscularis externa* - smooth muscle cells and collagen fibre layers. Note smooth-contoured nuclear membranes (arrows) of muscle cells.

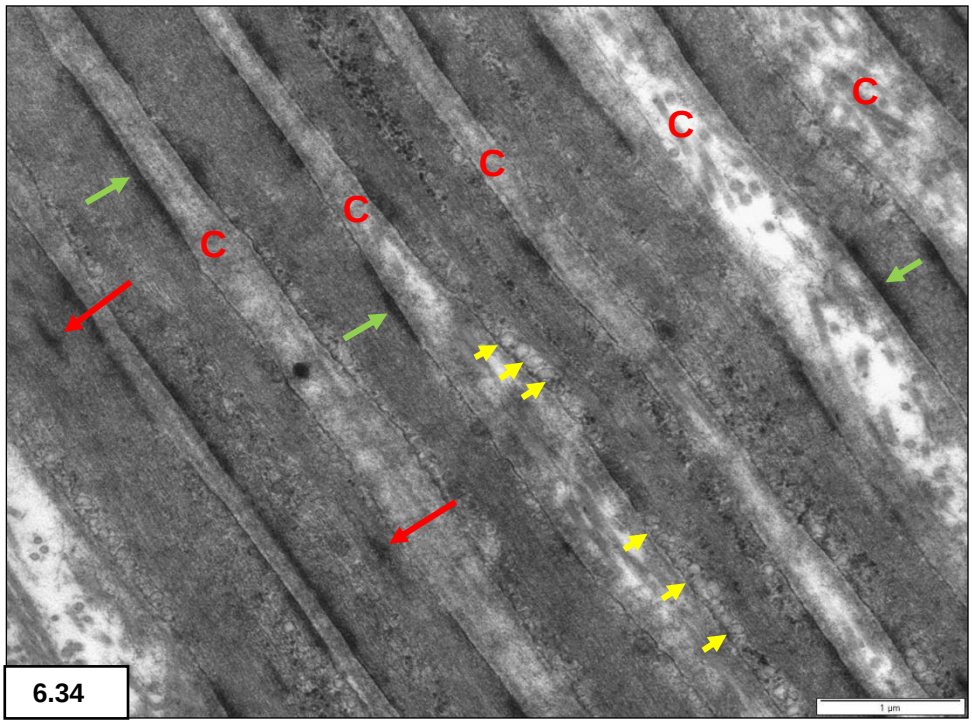

Figure 6.34: Intermediate filaments forming dense bodies (red arrows) and subplasmalemmal dense plaques (green arrows) in smooth muscle cells. Note cell surface pinocytotic vesicles (yellow arrows).Intervening collagen fibres (**C**).

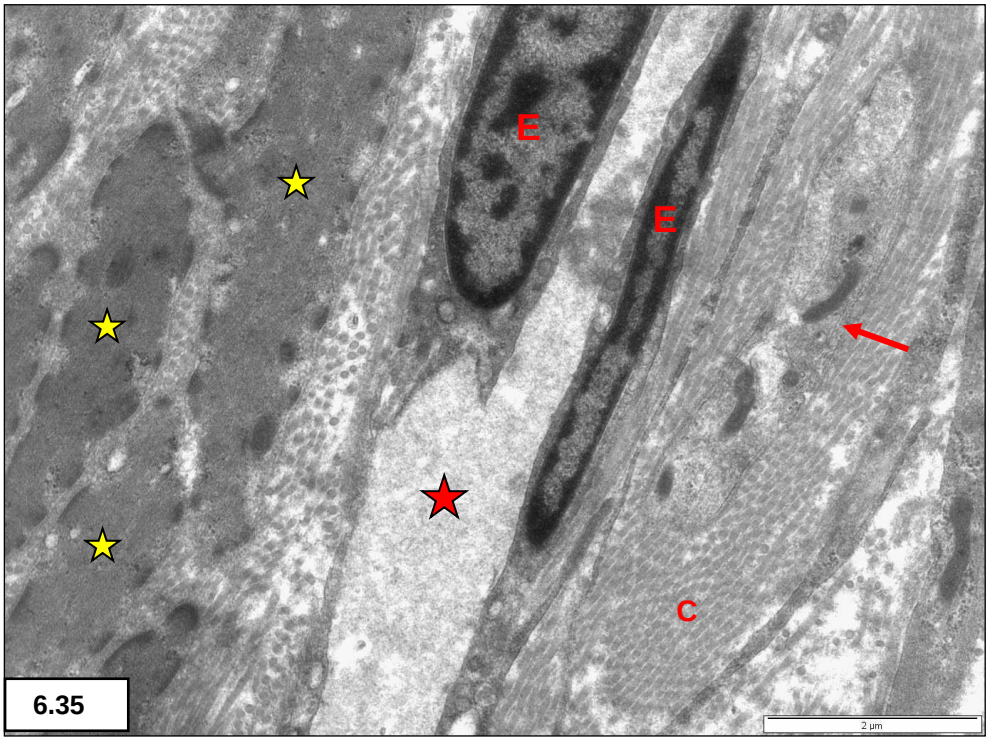

Figure 6.35: *Muscularis externa* - lymphatic vessel (red star), endothelial cells (**E**) smooth muscle cells (yellow stars) fibroblast (arrow). Collagen fibre (**C**).

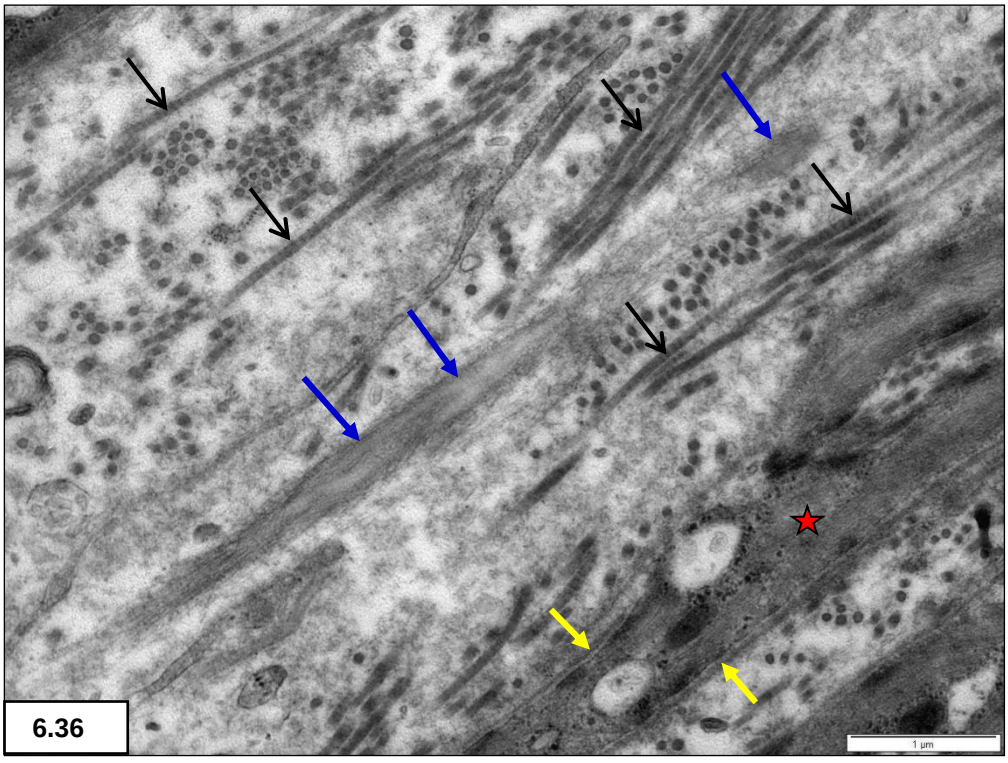

Figure 6.36: Elastic fibre (blue arrows), smooth muscle cell (star) surrounded by an external lamina (yellow arrows). Collagen fibrils (black arrows).

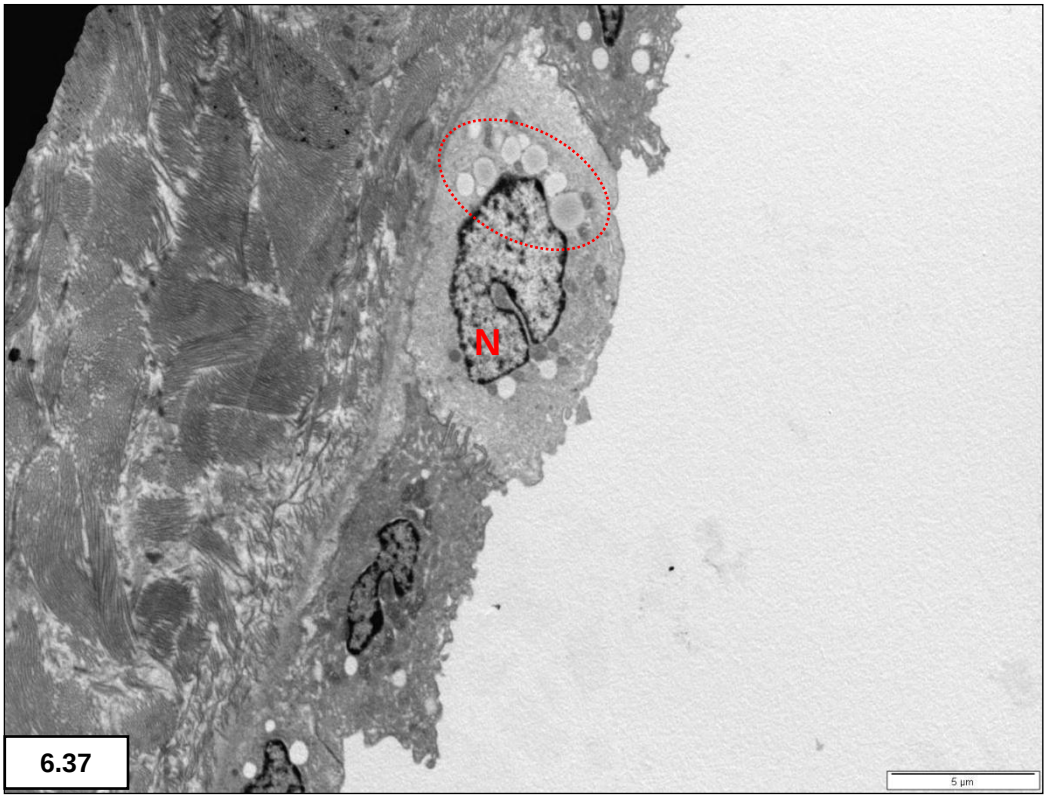

Figure 6.37: Serosa - dark and light staining mesothelial cells with clefted nuclei (**N**) and lipid droplets (dashed circle).

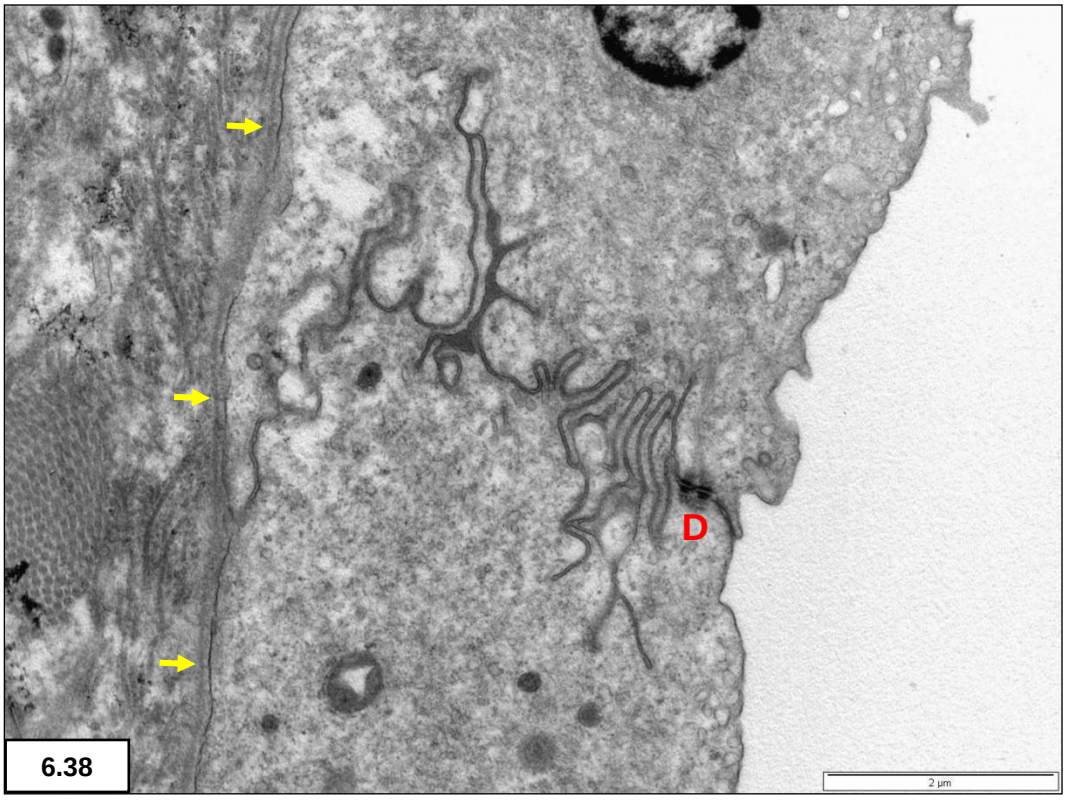

Figure 6.38: Interdigitations and desmosomes (D) between neighbouring mesothelial cells. Note the prominent basal lamina (arrows).

Figure 6.39: Serosa - large pinocytotic vesicles at the cell surface (bracket). Note lipid droplets (stars) and intermediate filaments (dashed circle).

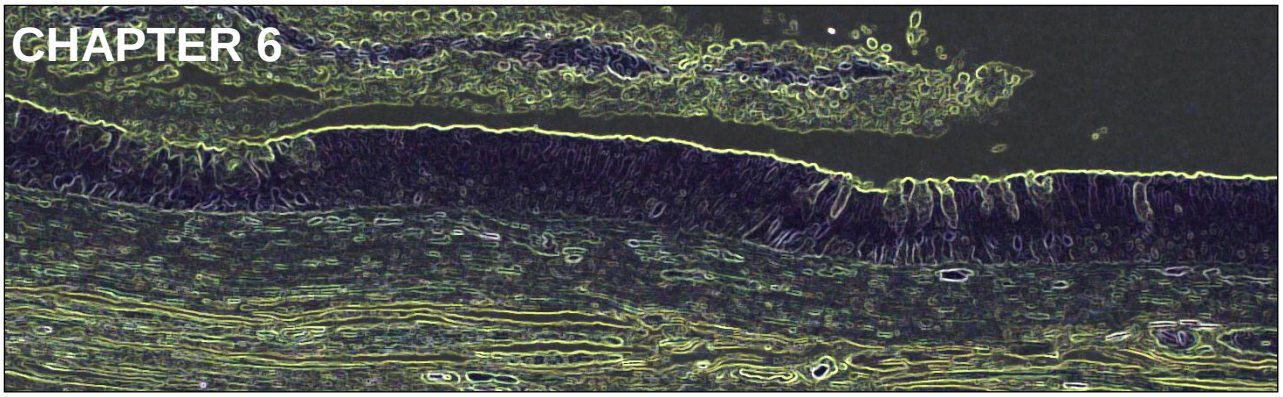

LIGHT MICROSCOPY AND TRANSMISSION ELECTRON MICROSCOPY OF THE GALLBLADDER

6.1 INTRODUCTION

Histology textbooks and internet websites cover the histology and transmission electron microscopy of the vertebrate gallbladder adequately (Ross *et al.* 2003; Junqueira *et al.* 1975; www.pathologyoutlines.com). A few publications contain merely superficial information regarding reptilian gallbladder histology (Schaffner 1998; Moura *et al.* 2009; McClellan-Green *et al.* 2006; Jacobson 2007). Silveira & Mimura (1999) gave more insight into the histology of the gallbladder of the snake *Bothrops jararaca.* Oldham-Ott & Gilloteaux (1997) reviewed the morphology, including light microscopy, transmission and scanning electron microscopy, of the gallbladder in amphibians, fish, reptiles (excluding crocodiles), birds and mammals. The authors found that although some morphological differences were present between vertebrates, their gallbladders were essentially similar and that reptilian gallbladders were morphologically the closest to the mammalian gallbladder. The literature is clearly lacking in microscopical descriptions of the gallbladder in crocodiles and observations on the Nile crocodile gallbladder will therefore unavoidably have to be compared to findings in other vertebrates.

6.2 LIGHT MICROSCOPY

6.2.1 MATERIALS AND METHODS

The gallbladders were separated from the perfused livers of five juvenile Nile crocodiles and their walls sampled from three different areas for immersion fixation in, namely near the cystic duct (neck), from the body and at the blind end (fundus). The samples were fixed in 10% acqueous buffered formalin for 24 hours to two weeks before dehydrating through a graded ethanol series, clearing in xylene and infiltrating with paraffin wax in a Shandon Excelsior Thermo Electron Corporation Tissue Processor. The samples were then embedded using a Thermolyne Histo Center 2 Embedding Unit and 3 to 5 micron thick sections were cut with a Reichert Jung rotary microtome. The following stains were used to demonstrate gallbladder architecture: haematoxylin & eosin (H/E; n=8), Periodic Acid-Schiff reaction (PAS; n=1) and PAS with diastase treatment (PAS-D; n=1) (Bancroft & Stevens 2003). Semi-thin toluidine blue stained resin sections (0.3 µm; n=54) were also examined to evaluate the appearance of the gallbladder at the light microscopy level (refer to section 6.3.1).

6.2.2 IMAGE CAPTURING & PROCESSING

Slides (n=64) were examined by brightfield illumination with an Olympus BX63 (Hamburg, Germany) compound microscope and images were recorded by an Olympus DP72 digital camera. The Olympus CellSense software, version 1.5, was used to adjust the brightness and contrast, and a sharpening filter was applied where required.

6.2.3 RESULTS

The gallbladder wall comprised three layers, namely, a mucosa that was subdivided into an epithelium and a *lamina propria*, a *muscularis externa* and a serosa, including a subserosa (Fig. 6.1).

The **mucosal epithelial layer** lined the gallbladder lumen and irregular shallow folding (Fig. 6.2) was apparent. In all three sampling zones the epithelium appeared to be composed of a mixture of simple and pseudostratified columnar epithelium. A single layer of basal nuclei indicated the presence of a simple columnar epithelium in certain areas whereas simple columnar epithelium merging with pseudostratified columnar epithelium

was present in other areas (Figs. 6.3 A & B). The epithelium presented with a combination of light and dark cells staining with the dark cells being slimmer and at times shorter than the neighbouring light cells (Fig. 6.4). The apical and basal cytoplasm was filled with PAS-positive (pink-staining) granules, giving these cells the appearance of slender goblet cells (Fig. 6.5). The fine granular PAS-positivity in the basal cytoplasm disappeared after diastase treatment (PAS-D) indicating the presence of glycogen (Fig. 6.6). The pink-staining apical granules remained, however, demonstrating their mucinous nature. Semi-thin toluidine blue resin sections revealed a faint pink metachromasia in the cytoplasm confirming the presence of mucin and glycogen (Fig. 6.7 B). Bulging of the epithelial cell apices (Figs. 6.8 A & B) were noted in some regions and other areas presented with exocytosis of secretory granules (Fig. 6.7 B) or a total loss of cell apices (Figs. 6.9 A & B). More dark cells were present in the areas where secretion or recovery was seen to be taking place (Fig. 6.7 A), and in one gallbladder large lipid-like globules (Fig. 6.9 B) were seen in the lumen next to the epithelium. Nuclei in the pseudostratified portions were arranged at different levels (Fig.6.10) in the basal third of the epithelium. Nucleoli, sometimes more than one per nucleus, were evident and a few had a distinctive red colour (Fig. 6.10). A few lymphocytes were present, mostly in the basal layer, with only some traversing the epithelium. Basal lymphocyte numbers were increased in areas of apical loss. Scanty large vacuolar areas were noted throughout the epithelium (Fig. 6.8 A). A PAS-positive basement membrane (Fig. 6.6) separated the epithelium from the ***lamina propria*** (Fig. 6.1) that consisted of blood vessels, lymphocytes and plasma cells in a collagenous stroma containing fibroblasts, collagen fibres and nerve ganglia. No glands were seen in this layer.

A ***muscularis externa*** (Fig. 6.1) was found external to the *lamina propria.* Smooth muscle cells (Fig. 6.9 B), with intervening collagen and fibroblasts, were seen at this level. Nerve ganglia, lymphatic and blood vessels were also present throughout the muscular layer.

The **serosa** (Fig. 6.11) consisted of a layer of simple squamous epithelium, the mesothelium, supported by a subserosa comprising connective tissue. Some mesothelial cells occasionally displayed a darker cytoplasm than others. Collagen fibres and blood vessels were present in the underlying connective tissue.

6.3 TRANSMISSION ELECTRON MICROSCOPY

6.3.1 MATERIALS AND METHODS

Parallel samples (n=15) of the three gallbladder zones were fixed in 2.5% glutaraldehyde in Millonig's buffer (pH 7.2), rinsed in Millonig's buffer, post-fixed in 1% osmium tetroxide in the same buffer, rinsed again and dehydrated through a series of graded ethanol before being infiltrated with propylene oxide and an epoxy resin and finally embedded in absolute epoxy resin. Tissue blocks were sectioned with a Reichert-Jung Ultramicrotome. Semi-thin resin sections (0.3 µm) were stained with 1% toluidine blue in borax and ultra-thin (50-90 nm) sections were collected onto copper grids (n=36) and stained with Reynold's lead citrate and an acqueous saturated solution of uranyl acetate (Hayat 2000).

6.3.2 IMAGE CAPTURING & PROCESSING

The grids (n=36) were examined with a Philips CM 10 transmission electron microscope (Eindhoven, Netherlands) operated at 80 kV. A Megaview III side-mounted digital camera was used to capture the images and the iTEM software (Olympus Soft Imaging System, GMBH) to adjust the brightness and contrast.

6.3.3 RESULTS

The **pseudostratified columnar epithelial cells** (see Figures 6.12 A & B) of the mucosa, revealed the following morphological features:

- Irregularly arranged apical microvilli, mostly uniform in shape and size, but a few with a staghorn, branching or club-shaped configuration (Fig. 6.14) and some being longer than others. Individual microvilli were covered by a glycocalyx.
- Apical junctional complexes (Figs. 6.15 & 6.17 B)
- Scanty cilia in a few cells, a single cilium per cell (Fig. 6.16)
- Desmosomes between deeper lateral cell borders (Fig. 6.22 A)
- Secretory granules (Figs. 6.13 & 6.17 A & B) containing mucus glycoproteins, mostly of medium electron density, but some more electron dense – found mostly in the apical cytoplasm, but also present in the basal portions of the cells

- Protrusions of the cytoplasm (Figs. 6.17 A & B), decapitation (pinching off) of apical cytoplasm (Figs. 6.19 A & B) and secretion of granule content into lumen (Figs. 6.18 A & B) – the microvilli were reduced or absent in these cells (Fig. 6.17 A & B)
- Lysosomes – some containing whorled membranes (Fig. 6.25)
- Apical and basal concentrations of mitochondria (Figs. 6.13 & 6.25) - the apical mitochondria was obscured in certain cells due to accumulations of secretory granules
- Golgi & granular endoplasmic reticulum (Fig. 6.22 B)
- Lipid-like globules in close association with the epithelial surface (Fig. 6.21)
- Monoparticulate glycogen particles, mostly seen in the basal cytoplasm (Fig. 6.24 A), but in a few instances (evident after release of secretory granules) in the subapical regions
- Scanty cytoplasmic calcium deposits (Fig. 6.26)
- Lateral (Figs. 6.22 A & B) and basolateral (Fig. 6.28) cell membrane interdigitations
- Intermediate filaments (Fig. 6.24 B)
- Large oval-shaped nuclei with smooth contours (Fig. 6.13)(in the resting phase), corrugated contours in active phase (Figs. 6.20 A & B)
- Distinctive round electron-dense nucleoli (comparable to red nucleoli seen in Figure 6.10) in some nuclei, in addition to 'normal' nucleoli – often the two different nucleoli were present in the same nucleus (Fig. 6.23)

Darker staining cells (Figs. 6.12 A & B), containing secretory granules and large collections of glycogen granules (Fig. 6.24 A), were present between lighter staining epithelial cells. The dark cells were slimmer than the light cells and some of them lacked secretory granules. The epithelial cells resembled slender goblet cells due to the accumulation of the subapical secretory granules (Fig. 6.13). The presence of the granules resulted in bulging of the cell apices into the gallbladder (Figs. 6.17 A & B). The luminal surface of these cells was almost devoid of microvilli. The secretory granules were seen to merge with the cytoplasmic membrane with release of their contents into the lumen (Figs. 6.18 A & B). In certain instances fusion of granules with resultant formation of large vacuoles seemed to take place before luminal release (Fig. 6.17 B). Loose-lying apical cellular structures containing secretory granules were similarly evident in the lumen (Fig. 6.19 B). Some cell apices were completely disrupted with the resultant loss of

cytoplasmic structures, leaving gaps in the epithelial lining (Figs. 6.20 A & B). Dark cells increased in number in areas of apical loss (Figs. 6.20 A & B) with the epithelium on occasion displaying only a single layer of dark basal nuclei. This finding dispelled the light microscopical impression that simple columnar epithelium co-existed with pseudostratified columnar epithelium. Occasional large cytoplasmic vacuoles, also seen light microscopically in the epithelium, filled with membranous debris (Fig. 6.27), were present in macrophages. A few lymphocytes were found in the basal epithelium and were also observed traversing the epithelium, with an increase of lymphocytes being noted in the regions of apical loss (Figs. 6.20 A & B). The epithelial cells rested on a continuous basal lamina that was mostly undulating (Fig. 6.28). Hemidesmosomes were identified where the cell membrane and basal lamina abutted (Fig. 6.28). The basal lamina seemed to be thickened underneath regions of apical loss (Fig. 6.29).

In the ***lamina propria,*** below the basal lamina, blood vessels and nerve ganglia (Fig. 6.31), surrounded by fibroblasts and sheets of collagen fibres, were present. The occasional eosinophil, plasma cell or lymphocyte was also found. Lymphocytes were more numerous in the vicinity of the basal lamina beneath areas of apical loss (Fig. 6.20 B). A few smooth muscle cells (Fig. 6.30), containing filaments forming densities and subplasmalemmal plaques, were seen between the collagen fibres. A small number of melanin granules (Fig. 6.32) were scattered among the collagen fibres in one gallbladder.

Subjacent to the *lamina propria* were prominent layers of alternating smooth muscle cells and collagen fibres (Fig. 6.33) which constituted the bulk of the **muscular layer**. However, the chief components were the smooth muscle cells that were mainly sectioned in the longitudinal plane. These cells were each surrounded by a thin, distinct external lamina and contained numerous intermediate filaments forming focal densities and subplasmalemmal dense plaques (Fig. 6.34). Elongated nuclei with mainly smooth contours were noted in the smooth muscle cells (Fig. 6.33). Many pinocytotic vesicles were identified at the cell surfaces. Scattered fragments of elastic fibres (Fig. 6.36), as well as lymphatic (Fig. 6.35) and blood vessels, were found lying between the smooth muscle cells and the collagen fibres. Nerve ganglia that occasionally included myelinated nerve fibres were present among the muscle cells.

The **serosa** consisted of a single layer of mesothelial cells (Fig.6.37) resting on an even basal lamina (Fig. 6.38). The cells contained indented nuclei and showed prominent

cytoplasmic interdigitations and desmosomes (Fig. 6.38) between neighbouring cells. Numerous large pinocytotic vesicles were located at the cell surfaces (Fig. 6.39). Cytoplasmic lipid droplets, mitochondria and intermediate filaments were present (Fig. 6.39).The cytoplasm of some cells was more electron-dense than others (Fig. 6.37) even though their ultrastructural features were similar. A connective tissue subserosa consisting of blood vessels surrounded by a collagenous stroma supported the basal lamina.

6.4 DISCUSSION

The gallbladder wall of reptiles is organised into an epithelial layer, a *lamina propria,* a muscular and a serosal layer (Gilloteaux 1997; Oldham-Ott & Gilloteaux 1997; Silveira & Mimura 1999) and was identical to that found in the juvenile Nile crocodile. As in other vertebrates a *muscularis mucosae* and submucosa (Junqueira *et al.* 1975; Ross *et al.* 2003; www.pathologyoutlines.com) were absent in the Nile crocodile gallbladder.

Several authors agree that the gallbladder **mucosa** of vertebrates, including reptiles, consists of either a simple or a pseudostratified columnar epithelium (Gilloteaux 1997; Oldham-Ott & Gilloteaux 1997; Schaffner 1998; Silveira & Mimura 1999; Moura *et al.* 2003; Mcclellan-Green *et al.* 2006; Jacobson 2007). Simple columnar epithelium could not be demonstrated in the juvenile Nile crocodile - the single layer of basal nuclei observed with the light microscope was seen with the electron microscope to be due to the loss of the apical cytoplasm. In higher vertebrates there is maturation of the gallbladder epithelium from pseudostratified in the embryo to simple high columnar epithelium in the adult (Silveira & Mimura 1999). Adult Nile crocodile gallbladders will need to be examined to establish whether the pseudostratified epithelium found in juveniles is merely a developmental stage.

Surface microvilli, junctional complexes and basolateral interdigitations correspond to the normal features of absorptive cells (Ross *et al.* 2003). The microvilli in this study were not as numerous or regular as those found in typical brush borders – the reason for the decrease in microvilli in the bulging apices is conceivably to allow for cell membrane permeability during exocytosis as described in the rabbit (Frederiksen *et al.* 1979). Single long microvilli were also found by Oldham-Ott and Gilloteaux (1997) in their study of the lizard gallbladder to which they ascribed a possible mechano- or chemo-sensory function. The scanty columnar brush cells found in the mouse (Luciano & Reale 1997) and in some

reptilian (Oldham-Ott and Gilloteaux 1997) gallbladders were not evident in the ultra-thin sections of the Nile crocodile gallbladder. Scanning electron microscopy however may reveal the presence of brush cells in this species. The cilia on the cell surface and the desmosomes situated between the deeper lateral cell borders observed in the present study were not mentioned in the cited publications. The fact that a single cilium per cell was seen in only a few cells may suggest a sensory role for these sparse cilia (Ross *et al.* 2003). Lipids are known to be absorbed from bile in human gallbladders (Hopwood & Ross 1997). In the present study the luminal lipid globules seen were possibly being absorbed by the epithelial cells and the large debris-filled vacuoles within the epithelium were perhaps a transient phase in the clearing of cellular remnants from the gallbladder lumen.

The goblet cell is not a normal constituent of the gallbladder epithelium in some mammals (Hayward 1962; www.pathologyoutlines.com), but its existence was briefly mentioned in reptiles (Oldham-Ott & Gilloteaux 1997; Schaffner 1998). The gallbladder epithelium of the juvenile Nile crocodile in the resting phase of the secretory cycle consisted in its entirety of slender goblet cells. The clustering of secretory granules in the subapical region of the Nile crocodile gallbladder epithelium is the first phase of the secretory cycle and comparable with the situation mentioned by Kuver *et al.* (2000) in the mouse gallbladder. The apical bulging, exocytosis of mucous granules and the stripping of the apical structures into the lumen are further sequential stages of the mucus secretory cycle (Lee 1980; Gilloteaux 1997; Oldham-Ott & Gilloteaux 1997; Kuver *et al.* 2000). There seems to be a combination of merocrine (exocytosis), apocrine (pinching off of apical cell cytoplasm) and to some extent holocrine (shedding of the whole cell containing cell product) secretion occurring in the Nile crocodile gallbladder epithelium. The lysosomes containing whorled membranes in the present study appeared similar to the myelinosomes described by Ghadially (1988). This author also refers to the secretory granules in alveolar cells as myelinosomes and perhaps the ‘lysosomes’ in the current study are rather precursor secretory granules. Glands, probably responsible for the mucus component in bile, were found in the *lamina propria* of mammals (Gilloteaux 1997) and in some reptiles (Oldham-Ott & Gilloteaux 1997), but were absent in Nile crocodile. The function of mucus production most likely belongs to the surface epithelial cells of the Nile crocodile gallbladder. The Nile crocodile gallbladder epithelium clearly has both absorptive and

secretory functions. This was also found to be true for mammalian gallbladders (Madrid *et al.* 1997).

Dark cells are known to appear in the normal human gallbladder epithelium and there is speculation that this is due to cellular dehydration (Ghadially 1998). The finding of dark cells among the lighter epithelial cells in the Nile crocodile epithelium is in agreement with this inference as active fluid transport for bile concentration supposedly occurs from the lumen across the gallbladder epithelium. Dark cells may also be a forerunner of dying cells (Ghadially 1998) and in the present study this may be the reason for the proliferation of dark cells in areas of secretory activity, i.e. perhaps the dark cells die off after secretion. In contrast to this deduction, large areas of the epithelium consisted only of dark basal nuclei in sections of total apical loss – possibly these cells act as stem cells to balance cell turnover. Ross *et al.* (2003) explained that in certain pseudostratified epithelia the basal cells are stem cells that produce the functional epithelial cells thus balancing cell turnover. Lamote & Willems (1997) found that the normal gallbladder has a low cell turnover rate, but that abnormal circumstances could trigger proliferative activity. The nucleoli found in the nuclei of human gallbladder epithelium were described as indistinct (www.pathologyoutlines.com), but those of the Nile crocodile were very distinctive in their round shape and intense, uniform electron-density.

The increase of lymphocytes in the basal epithelium as well as in the underlying *lamina propria* in regions of apical loss may be a defense mechanism in a compromised epithelium. Concomitant with this deduction is the thicker basal lamina in these regions that may serve to strengthen the gallbladder wall. The presence of a thicker basal lamina was not cited by other authors, but Hopwood & Ross (1997) mentioned the importance of basement membranes allowing the movement of regenerating cells during tissue renewal.

Gilloteaux (1997) mentioned the presence of nerve ganglia between the fibromuscular and the subserosal layers in the vertebrate gallbladder – in the Nile crocodile nerve ganglia were also present in the ***lamina propria***. Melanin is known as a free radical trap in reptilian livers (McClellan-Green *et al.* 2006) and the free-lying melanin granules found between the collagen fibrils in this study may function in this regard. Glands that are variably present in this layer in other vertebrates (Gilloteaux 1997) were not seen in the Nile crocodile.

The present ultrastructural report of the smooth muscle cells in the **muscular layer** of the Nile crocodile gallbladder is almost identical to the description of smooth muscle cells given by Ghadially (1998), the only exception being the smooth-contoured nuclear outline. Ghadially (1998) also described these nuclei as folded, notched or showing many invaginations. Fragmented elastic fibres were found between the muscle-collagen layers in the *muscularis externa*, but their existence was not specified in other reptiles. In humans elastic tissue was noted in the subserosal layer (www.pathologyoutlines.com). Rokitansky-Aschoff crypts and the Canals of Luschka seen in the fibromuscular layer of other vertebrates (Gilloteaux 1997) were absent in the Nile crocodile gallbladder sections examined.

Descriptions (Junqueira *et al.* 1975; Ross *et al.* 2003) of the **serosa** are limited to the mere mentioning of connective tissue, blood and lymphatic vessels covered by a simple squamous epithelium. The serosa and subserosa in the Nile crocodile gallbladder is similar to the general vertebrate pattern.

6.5 REFERENCES

BANCROFT, J.D. & STEVENS, A. 2003. *Theory and practice of histological techniques.* Churchill Livingstone, New York.

FREDERIKSEN, O., MØLLGÅRD, K. & ROSTGAARD, J. 1979 Lack of correlation between transepithelial transport capacity and paracellular pathway ultrastructure in alcian blue-treated rabbit gallbladders. *Journal of Cell Biology,* 83: 383-393.

GHADIALLY, F.N. 1988. *Ultrastructural pathology of the cell and matrix.* Butterworths, London.

GILLOTEAUX, J. 1997. Introduction to the biliary tract, the gallbladder, and gallstones. *Microscopy Research and Technique,* 38: 547-551.

HAYAT, M.A. 2000. *Principles and techniques of electron microscopy: biological applications.* Cambridge University Press, Cambridge, UK.

HAYWARD, A. F. 1962. Aspects of the fine structure of the gallbladder epithelium of the mouse. *Journal of Anatomy,* 96: 227-236.

HOPWOOD, D. & ROSS, P.E. 1997. Biochemical and morphological correlations in human gallbladder with reference to membrane permeability. *Microscopy Research and Technique,* 38: 631– 642.

JACOBSON, E.R. 2007. Overview of reptile biology, anatomy, and histology, in *Infectious diseases and pathology of reptiles,* edited by E.R. Jacobson. CRC Press, Taylor & Francis Group, 6000 Broken Sound Parkway NW, Suite 300, Boca Raton, FL 33487-2742, pp. 1-130.

JUNQUEIRA, L.C., CARNEIRO, J & CONTOPOULUS, A.N. 1975. *Basic histology.* Lange Medical Publications, Los Altos, California.

KUVER, R., KLINKSPOOR, J.H., OSBORNE, W.R.H. & LEE, S.P. 2000. Mucous granule exocytosis and CFTR expression in gallbladder epithelium. *Glycobiology,* 10: 149-157.

LAMOTE, J. & WILLEMS, G. 1997. DNA synthesis, cell proliferation index in normal and abnormal gallbladder epithelium. *Microscopy Research and Technique,* 38: 609–615.

LEE, S. P. 1980. The mechanism of mucus secretion by the gallbladder epithelium. *British Journal of Experimental Pathology*, 61: 117-119.

LUCIANO, L. & REALE, E. 1997. Presence of brush cells in the mouse gallbladder. *Microscopy Research and Technique,* 38:598–608.

MADRID, J.F., HERNANDEZ, F. & BALLESTA, J. 1997. Characterization of glycoproteins in the epithelial cells of human and other mammalian gallbladder. A review. *Microscopy Research and Technique,* 38: 616–630.

MCCLELLAN-GREEN, P., CELANDER, M. & OBERDÖRSTER, E. 2006. Hepatic, renal and adrenal toxicology, in *Toxicology of reptiles,* edited by S.C. Gardner & E. Oberdörster. CRC Press, Taylor & Francis Group, 6000 Broken Sound Parkway NW, Suite 300, Boca Raton, FL 33487-2742, pp. 123-148.

MOURA, L.R., SANTOS, A.L.Q., BELLETI, M.E., VIEIRA, L.G., ORPINELLI, S.R.T. & DE SIMONE, S.B.S. 2009. Morphological aspects of the liver of the freshwater turtle *Phrynops geoffroanus* Schweigger, 1812 (Testudines, Chelidae). *Brazilian Journal of Morphological Science,* 26: 129-134.

OLDHAM-OTT, C.K. & GILLOTEAUX, J. 1997. Comparative morphology of the gallbladder and biliary tract in vertebrates: variation in structure, homology in function and gallstones. *Microscopy Research and Technique,* 38: 571-597.

ROSS, M.H., KAYE, G.I. & PAWLINA, W. 2003. *Histology: a text and atlas.* 4th ed. Lippincott Williams & Wilkens, Baltimore, USA.

SCHAFFNER, F. 1998. The hepatic system, in *Biology of reptilia: volume 19, Morphology G: Visceral organs,* edited by C. Gans & A.B. Gaunt. Society for the Study of Amphibians and Reptiles, Missouri, pp. 485-531.

SILVEIRA, P.F. & MIMURA, O.M. 1999. Concentrating ability of the *Bothrops jararaca* gallbladder. *Comparative Biochemistry and Physiology,* Part A, 123: 25–33.

WWW site references:

www.pathologyoutlines.com